NAVAL POSTGRADUATE SCHOOL

MONTEREY, CALIFORNIA

THESIS

EXTRACTION OF A WEAK CO-CHANNEL INTERFERING COMMUNICATION SIGNAL USING COMPLEX INDEPENDENT COMPONENT ANALYSIS

by

Matthew E. Hagstette

June 2013

Thesis Advisor:	Monique P. Fargues
Co-Advisor:	Roberto Cristi

Approved for public release; distribution is unlimited

THIS PAGE INTENTIONALLY LEFT BLANK

REPORT DOCUMENTATION PAGE			*Form Approved OMB No. 0704-0188*
Public reporting burden for this collection of information is estimated to average 1 hour per response, including the time for reviewing instruction, searching existing data sources, gathering and maintaining the data needed, and completing and reviewing the collection of information. Send comments regarding this burden estimate or any other aspect of this collection of information, including suggestions for reducing this burden, to Washington headquarters Services, Directorate for Information Operations and Reports, 1215 Jefferson Davis Highway, Suite 1204, Arlington, VA 22202-4302, and to the Office of Management and Budget, Paperwork Reduction Project (0704-0188) Washington DC 20503.			
1. AGENCY USE ONLY *(Leave blank)*	**2. REPORT DATE** June 2013	**3. REPORT TYPE AND DATES COVERED** Master's Thesis	
4. TITLE AND SUBTITLE EXTRACTION OF A WEAK CO-CHANNEL INTERFERING COMMUNICATION SIGNAL USING COMPLEX INDEPENDENT COMPONENT ANALYSIS			**5. FUNDING NUMBERS**
6. AUTHOR(S) Matthew E. Hagstette			
7. PERFORMING ORGANIZATION NAME(S) AND ADDRESS(ES) Naval Postgraduate School Monterey, CA 93943-5000			**8. PERFORMING ORGANIZATION REPORT NUMBER**
9. SPONSORING /MONITORING AGENCY NAME(S) AND ADDRESS(ES) N/A			**10. SPONSORING/MONITORING AGENCY REPORT NUMBER**
11. SUPPLEMENTARY NOTES The views expressed in this thesis are those of the author and do not reflect the official policy or position of the Department of Defense or the U.S. Government. IRB Protocol number ____N/A____.			
12a. DISTRIBUTION / AVAILABILITY STATEMENT Approved for public release; distribution is unlimited			**12b. DISTRIBUTION CODE**

13. ABSTRACT (maximum 200 words)

Independent Component Analysis (ICA) has largely been applied to the biomedical field over the past two decades and only recently extended to the processing of complex non-circular sources. The feasibility and performance of complex ICA to extract a weak co-channel interfering communications signal from a television broadcast signal is investigated in this thesis. The performance of three algorithms, complex maximization of non-Gaussianity (CMN) by Novey et al., RobustICA by Zarzoso et al., and complex fixed-point algorithm (CFPA) by Douglas, over varied interference-to-noise ratios (INR) for a fixed signal-to-interference ratio (SIR) is obtained by simulation.

The communication signals examined for the weak interferer are binary phase-shift keying (BPSK), four-level rectangular quadrature amplitude modulation (4-QAM), and 16-level rectangular quadrature amplitude modulation (16-QAM), and the television broadcast signals are North American standard, Advanced Television Systems Committee (ATSC) and European standard, Digital Video Broadcasting - Terrestrial (DVB-T). Improved performance and sensitivity to the prewhitening step present in the ICA implementations are shown as the number of sensors increases.

14. SUBJECT TERMS Complex Independent Component Analysis (ICA), Co-channel interference			**15. NUMBER OF PAGES** 71
			16. PRICE CODE
17. SECURITY CLASSIFICATION OF REPORT Unclassified	**18. SECURITY CLASSIFICATION OF THIS PAGE** Unclassified	**19. SECURITY CLASSIFICATION OF ABSTRACT** Unclassified	**20. LIMITATION OF ABSTRACT** UU

NSN 7540-01-280-5500

Standard Form 298 (Rev. 2-89)
Prescribed by ANSI Std. 239-18

THIS PAGE INTENTIONALLY LEFT BLANK

Approved for public release; distribution is unlimited

EXTRACTION OF A WEAK CO-CHANNEL INTERFERING COMMUNICATION SIGNAL USING COMPLEX INDEPENDENT COMPONENT ANALYSIS

Matthew E. Hagstette
Lieutenant, United States Navy
B.S., Louisiana State University, 2003
M.B.A., Charleston Southern University, 2007
M.S., National University of Singapore, 2013

Submitted in partial fulfillment of the
requirements for the degree of

MASTER OF SCIENCE IN ELECTRICAL ENGINEERING

from the

NAVAL POSTGRADUATE SCHOOL
June 2013

Author: Matthew E. Hagstette

Approved by: Monique P. Fargues
Thesis Advisor

Roberto Cristi
Co-Advisor

R. Clark Robertson
Chair, Department of Electrical and Computer Engineering

THIS PAGE INTENTIONALLY LEFT BLANK

ABSTRACT

Independent Component Analysis (ICA) has largely been applied to the biomedical field over the past two decades and only recently extended to the processing of complex non-circular sources. The feasibility and performance of complex ICA to extract a weak co-channel interfering communications signal from a television broadcast signal is investigated in this thesis. The performance of three algorithms, complex maximization of non-Gaussianity (CMN) by Novey et al., RobustICA by Zarzoso et al., and complex fixed-point algorithm (CFPA) by Douglas, over varied interference-to-noise ratios (INR) for a fixed signal-to-interference ratio (SIR) is obtained by simulation.

The communication signals examined for the weak interferer are binary phase-shift keying (BPSK), four-level rectangular quadrature amplitude modulation (4-QAM), and 16-level rectangular quadrature amplitude modulation (16-QAM), and the television broadcast signals are North American standard, Advanced Television Systems Committee (ATSC) and European standard, Digital Video Broadcasting - Terrestrial (DVB-T). Improved performance and sensitivity to the prewhitening step present in the ICA implementations are shown as the number of sensors increases.

THIS PAGE INTENTIONALLY LEFT BLANK

TABLE OF CONTENTS

THIS PAGE INTENTIONALLY LEFT BLANK

LIST OF FIGURES

LIST OF TABLES

THIS PAGE INTENTIONALLY LEFT BLANK

LIST OF ACRONYMS AND ABBREVIATIONS

ATSC	Advanced Television Systems Committee
BER	Bit Error Rate
BPSK	Binary Phase Shift Key
BSS	Blind Source Separation
Cdf	Cumulative distribution function
cFastICA	Complex FastICA
CFPA	Complex Fixed-Point Algorithm
CI	Confidence Interval
CMN	Complex Maximization of Non-Gaussianity
DVB-T	Digital Video Broadcasting – Terrestrial
EVD	Eigenvalue Decomposition
FFT	Fast Fourier Transform
ICA	Independent Component Analysis
IID	Independent and Identically Distributed
INR	Interference-to-Noise Ratio
OFDM	Orthogonal Frequency-Division Multiplexed
PCA	Principal Component Analysis
Pdf	Probability density function
QAM	Quadrature Amplitude Modulation
SER	Symbol Error Rate
SIR	Signal-to-Interference Ratio
SVD	Singular Value Decomposition

THIS PAGE INTENTIONALLY LEFT BLANK

EXECUTIVE SUMMARY

In this work, we investigate the co-channel interference problem where a weak communication signal is imbedded in the same channel as a much stronger broadcast signal in the presence of noise, and we desire to recover the weak signal. This problem has relevance both in commercial communication and defense-related applications such as unintentional or intentional jamming and passive surveillance. Independent component analysis (ICA) has been shown to be well suited for co-channel signal separation applications and is the approach selected to investigate this problem.

Independent component analysis refers to the separation of signals from a set of mixtures when the mixture process is unknown and the sources are independent. Most early ICA-based approaches were derived for real source environments. Until the last few years, extensions to the complex source cases did not take into consideration potential complex non-circular source properties. However, recently developed algorithms taking into account complex non-circular source properties have been shown to lead to increased performance when the sources under investigation fit such criteria. Most complex communication signals exhibit non-circular properties, and three ICA algorithms are considered to extract a weak co-channel interfering communication signal from a television broadcast signal with the assumption of no multipath: complex maximization of non-Gaussianity (CMN) by Novey et al. [1], RobustICA by Zarzoso et al. [2], and complex fixed-point algorithm (CFPA) by Douglas [3]. Each ICA algorithm separates the signals by maximizing the non-Gaussianity of the source signals. The CMN algorithm uses an information theory based, quasi-Newton optimization approach through maximization of negentropy, which is estimated through nonlinear functions. The remaining algorithms are both kurtosis based approaches. RobustICA employs an exact line search optimization to maximize/minimize kurtosis, while CFPA uses a quasi-Newton optimization technique.

The dominant signal considered in the study is a television broadcast signal. Two standards were considered: North American ATSC (Advanced Television Systems Committee) standard and European DVB-T (Digital Video Broadcasting – Terrestrial)

standard. The ATSC broadcast is an eight-level amplitude-shift keying (8-ASK) signal, while the DVB-T broadcast is an orthogonal frequency-division multiplexed (OFDM) four-level rectangular quadrature amplitude modulation (4-QAM), 16-level rectangular quadrature amplitude modulation (16-QAM), or 64-level rectangular quadrature amplitude modulation (64-QAM) signal. The 4-QAM OFDM option was chosen for the simulations. The types of weak communication signals imbedded in the TV signal were binary phase shift keying (BPSK), 4-QAM, and 16-QAM.

With no noise, extraction of the weak signal occurred without errors at signal-to-interference (SIR) ratios ranging from –50 to 60 dB for the two-sensor case. When the mixtures are proper, i.e., the same number of signals as channels, the ICA algorithms lead to exact recovery of the weak signal. To further illustrate this point, the number of sensors was increased to three and same noise added to each channel for a total of three mixtures and three signals. Again, the ICA algorithms extracted the weak signal without errors. With different noise sequences added to each channel instead, the problem can be viewed as under-determined with a ratio of K:(K+2), where K is the number of sensors. When the number of sensors increases without any noise present, the problem can be viewed as over-determined with a ratio of K:2. In this case, all three algorithms become numerically unstable and fail to extract the weak signal in the no-noise case when more than two sensors are used and a prewhitening step is applied in the ICA process. However, when no prewhitening step is applied, extraction occurs with only minor errors using RobustICA.

We investigated what impact the level of separation between signals mixtures has on the weak signal extraction performance in the two-sensor case. To that end, all channel coefficients, except for one of the channel coefficients associated with the weak signal, were fixed to 1.0, and the phase of the last coefficient was selected to be either $\pi/8$, $\pi/2$, or π for various interference-to-noise ratios (INR) and SIR = 30 dB. Results show the extraction performance increases as the channel coefficient phase angle increases as a result of the increase in mixture separation.

We also examined the effects of using multiple sensors. Note that it is desirable to stop the extraction process as quickly as possible when more than two sensors are used

since only the weak communication signal is of interest here. In order to do so, we show that the weak signal is always successfully extracted as one of the first two components except in cases where the recovery quality is too poor to be considered successful. As a result, all implementations were stopped after the extraction of the first two signals when considering more-than-two-sensor cases.

For all algorithms considered, results show the overall extraction performance increases as the number of sensors increases. However, at higher number of sensors and low levels of noise, the underdetermined K:(K+2) scenario tends to behave as the over-determined K:2 case, leading to ill-conditioned behavior when prewhitening is applied. Although there is a slight reduction in performance, this instability is not present when the mixtures are not prewhitened.

Overall results show ICA as a viable option to extract a weak co-channel interfering communication signal with no multipath. Findings show a dependency on the level of signal mixtures separation. All algorithms also show improved extraction performance as the number of sensors increases but also show sensitivity to prewhitening in low noise levels for cases with high number of sensors.

LIST OF REFERENCES

[1] M. Novey and T. Adalı, “Complex ICA by negentropy maximization,” IEEE Trans. Neural Networks, vol. 19, no. 4, pp. 596–609, Apr. 2008.

[2] S. C. Douglas, “Fixed-point algorithms for the blind separation of arbitrary complex-valued non-Gaussian signal mixtures,” EURASIP Journal on Advances in Signal Processing, 2007, DOI: 10.1155/2007/36525.

[3] V. Zarzoso and P. Comon, “Robust independent component analysis by iterative maximization of the kurtosis contrast with algebraic optimal step size,” IEEE Trans. Neural Networks, vol. 21, no. 2, pp. 248–261, Feb. 2010.

THIS PAGE INTENTIONALLY LEFT BLANK

ACKNOWLEDGMENTS

I would like to thank Professor Fargues for her help and guidance during this process. Working with her made this a welcoming and rewarding experience. I would also like to thank the faculty of the ECE department for their support.

THIS PAGE INTENTIONALLY LEFT BLANK

I. INTRODUCTION

In this work, we investigate the co-channel interference problem where a weak communication signal is imbedded in the same channel as a much stronger broadcast signal in the presence of noise. Classical filtering schemes that typically separate signals based on frequencies are not considered since the two signals of interest share the same frequency range. Instead, we choose to explore the use of independent component analysis (ICA) to extract the weak signal. This problem has relevance both in commercial communication and defense-related applications such as unintentional or intentional jamming and passive surveillance.

Initial applications of ICA began in the early 1980s as a model for mapping muscle contractions to neurological signals. Earlier approaches were algebraic methods based on second and fourth order cumulants, with very limited applications outside of the neural network field. It was not until the mid-1990s, when approaches involving statistical optimization were proposed, that ICA started to become an established field of research [1]. Algorithms by Bell et al. [2] and Comon [3] were some of the first approaches which subsequently were extended to the FastICA algorithm by Hyvärinen et al. [4]. Independent component analysis has proved remarkably successful in the biomedical field to extract signals collected with multi-electrode devices. Examples include fetal electrocardiogram extraction, electromyography, electroencephalography, and functional magnetic resonance imaging [5]. These signals benefit from being mathematically real-valued, which allows for simplifications to be made in the implementations.

More recently ICA has been applied to the communications field. However, many communication signals are inherently complex-valued and non-circular in nature which adds an additional level of complexity. Initial ICA algorithms derived for real-valued signals were first extended to the complex domain without taking into account the potential non-circular nature of the complex signals investigated. As a result, recently developed ICA algorithms taking into consideration potential non-circular properties of the complex signals investigated were introduced and have shown improved performances [6, 7, 8].

In this work we consider the following three ICA algorithm derived for complex, non-circular signals: complex maximization of non-Gaussianity (CMN) by Adali et al. [6], the complex fixed-point algorithm (CFPA) by Douglas [7], and the RobustICA by Zarzoso et al. [8]. We applied these algorithms to extract a weak co-channel communication signal imbedded in a strong television (TV) broadcast signal with no multipath present.

This thesis is organized in the following manner. We begin by introducing ICA concepts in Chapter II. The concept of prewhitening, different types of ICA approaches proposed over the years and their limitations, and issues involving complex signals are also discussed. An overview of the three complex ICA algorithms evaluated in this work is presented in Chapter III. The experimental setup and model description are detailed in Chapter IV, while a discussion of the results is presented in Chapter V. Finally, summary and possibilities for follow-on work is provided in Chapter.

II. STATISTICAL CRITERIA AT THE BASIS OF BLIND SOURCE SEPARATION

A. BLIND SOURCE SEPARATION

In general terms, Blind Source Separation (BSS) refers to the separation of signals from a set of mixtures when little is known about the sources or the mixture process. It is accomplished by applying a transform to the set of signal mixtures which decomposes the mixtures into a vector space, which in turn maximizes some user-defined separation criteria. Some popular methods included in this class of separation techniques are adaptive filtering, low-complexity coding and decoding, principal component analysis (PCA), and independent component analysis. Both PCA and ICA are techniques applicable to the co-channel interference problem.

B. PCA

Principle component analysis can be used to remove information redundancy between observed mixtures contained in the correlation between the mixtures. The answer to the PCA problem is given by a transform consisting of the eigenvector solution to the covariance matrix $\mathbf{C}_{\mathbf{x}}$ of the zero-mean mixtures $\mathbf{x}$ of length N [9]

$$\mathbf{C}_{\mathbf{x}} = \frac{1}{N}\mathbf{x}\mathbf{x}^{H} = \mathbf{Q}\Omega\mathbf{Q}^{H}, \tag{1}$$

where $(.)^{H}$ is the complex conjugate transpose operator, $\mathbf{Q}$ contains the eigenvectors, and Ω is a diagonal matrix with the eigenvalues on its main diagonal. The result of the applied transform is the decomposition of the mixtures into orthogonal components $\tilde{\mathbf{z}}$ given by

$$\tilde{\mathbf{z}} = \mathbf{Q}^{H}\,\mathbf{x}. \tag{2}$$

The significance of each component is related to the eigenvalue of the associated eigenvector [9]. The component with the largest eigenvalue has the largest variance and, therefore, contains the most information. One application of PCA is data compression. When PCA is applied to a large data set with high redundancy, the data set can be reduced in size with minimal information loss by keeping the contributions due to the

eigenvectors associated with larger eigenvalues and neglecting others. The neglected components in this situation provide little to no information.

For the co-channel interference problem, under the assumption that the signals of interest are non-Gaussian in distribution and independent, PCA cannot be used alone to extract independent signals since it only decorrelates the signal mixtures. More is needed to extract signals which are independent. However, PCA is beneficial in ICA as a preprocessing technique, termed whitening, to remove the effects of first and second-order statistics which simplifies the resulting ICA process [9]. A zero-mean random vector is said to be whitened when its components are uncorrelated and have unit variance. Therefore, PCA is used to decorrelate the signal mixtures which are then scaled to unit variance. The whitened signal mixtures $\mathbf{z}$ are given by

$$\mathbf{z} = \Omega^{-1/2} \mathbf{Q}^H \mathbf{x}. \tag{3}$$

Prewhitening can also be performed using the singular value decomposition (SVD),

$$\mathbf{x} = \mathbf{U}\mathbf{D}\mathbf{V}^H. \tag{4}$$

Here $\mathbf{U}$ is the unitary left singular vector matrix which can be shown to be identical to the eigenvectors matrix obtained for $\mathbf{x}\mathbf{x}^H$, $\mathbf{V}$ is the unitary right singular vector matrix which can be shown to be identical to the eigenvectors matrix obtained for $\mathbf{x}^H\mathbf{x}$, and $\mathbf{D}$ is the diagonal singular value matrix containing the square root of the eigenvalues for both $\mathbf{x}\mathbf{x}^H$ and $\mathbf{x}^H\mathbf{x}$. Recall Ω is the diagonal matrix containing the eigenvalues of $\mathbf{x}\mathbf{x}^H/N$. Therefore, Ω is equal to $\mathbf{D}^2/N$, and since $\mathbf{Q}$ and $\mathbf{U}$ are identical, by substituting (4) into (3) the whitened signal mixtures using SVD can be shown to be

$$\mathbf{z} = \sqrt{N}\ \mathbf{V}^H. \tag{5}$$

Note that prewhitening using the eigenvalue decomposition (EVD) involves an inverse operation where using SVD does not. For this reason algorithms utilizing the EVD in the prewhitening step were altered to use the SVD method instead to avoid numerical instability for cases leading to very small eigenvalues.

C. ICA

In addition to PCA, ICA assumes the source signals of the mixture are not only uncorrelated but also statistically independent. For the real case, the linear ICA model is described by

$$\mathbf{x} = \mathbf{A}\,\mathbf{s}, \tag{6}$$

where $\mathbf{x} = (s_1, \ldots, s_N)^T$ contains the N source signals, $\mathbf{A}$ is a N × P mixing matrix, and $\mathbf{x} = (x_1, \ldots, x_P)^T$ contains the P observed channel mixtures. The objective of ICA is to find an un-mixing matrix $\mathbf{W}$ which recovers an estimate of the N source signals $\mathbf{y} = (y_1, \ldots, y_N)^T$ as defined by

$$\mathbf{y} = \mathbf{W}\,\mathbf{x}. \tag{7}$$

The matrix $\mathbf{W}$ consists of N un-mixing vectors with P elements, $\mathbf{w} = (w_{N1}, w_{N2}, \ldots, w_{NP})^T$. One un-mixing vector is used to extract one source signal:

$$y = \mathbf{w}^T\,\mathbf{x}. \tag{8}$$

The mixing and un-mixing of a simple two-source and two-sensor case is illustrated in Figure 1.

The underlying assumption behind ICA algorithms is independence between the source signals. Since the mixing operation is a linear transformation, the mixtures of the independent source signals are correlated. Although the mixtures from one channel to the next are correlated, the components of each channel mixture are still independent, which leads to the optimal un-mixing vector being orthogonal to the span of all other transformed components. One source signal is extracted by taking the inner product between this optimal un-mixing vector and the observed mixtures. The source signals can be extracted individually with one un-mixing vector or simultaneously with the matrix of un-mixing vectors $\mathbf{W}$. Searching for the un-mixing vectors is where different approaches arise. That search can be achieved through the maximization or minimization of specific signal attributes, which in turn maximizes the independence between the estimated source signals.

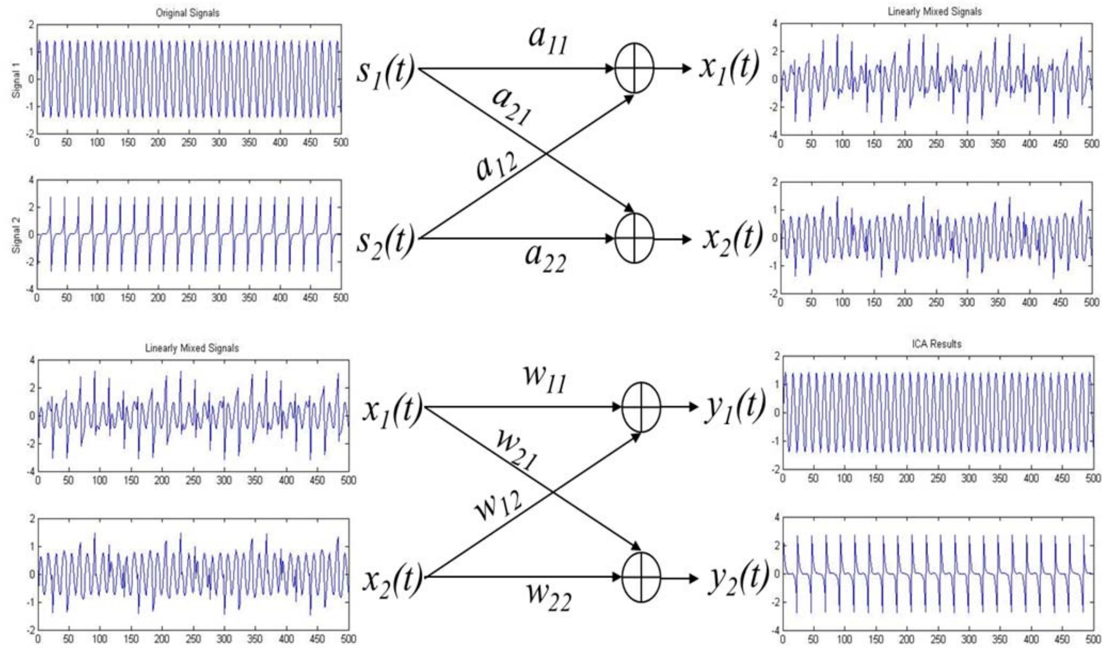

Figure 1. Example of the mixing and un-mixing of a two-source and two-sensor case using ICA.

D. MAXIMIZING INDEPENDENCE

Two common approaches to maximize the independence of the estimated source signals are through information theory based methods or by maximizing a measure of non-Gaussianity of the density of the estimated source signals. The following sections describe three approaches to maximize the independence of the estimated source signals.

1. Information-maximization

Information-maximization, also known as Infomax, is an ICA technique suggested in 1995 by Bell, et al. for neural networks applications [2]. Its overall objective is to extract independent signals by minimizing the mutual information between those signals, which is accomplished through the maximization of the joint signal entropy. The entropy of the source signal is defined as

$$H(y) = -\int_{-\infty}^{\infty} p(y)\log p(y)\,dy, \tag{9}$$

where $p(y)$ is the probability density function (pdf) of the signal. The relationship between the joint entropy $H(y_1, y_2)$ of two signals y_1 and y_2 and the mutual information shared between the two signals $I(y_1, y_2)$ is described by

$$H(y_1, y_2) = H(y_1) + H(y_2) - I(y_1, y_2). \tag{10}$$

Infomax uses the fact that when a random variable $y \in [0,1]$ is transformed by its cumulative distribution function (cdf) $G(y)$, the resulting random variable is uniformly distributed between zero and one. Note that a random variable with a uniform distribution has the maximum entropy among all variables in the same range [2]. Furthermore, since the cdf is monotonic in nature, $G(y)$ is an invertible function, and the independence of the estimated source signals is maximized when the entropy of their transform is at a maximum. Estimated source signals obtained via ICA can be written in terms of the un-mixing vectors and signal mixtures. Therefore, the basis of Infomax is to find the un-mixing vector which maximizes the individual entropy of the transformed estimated source signal $G(\mathbf{w}^T\mathbf{x})$, which in turn minimizes the mutual information between the estimated source signal and the remaining signals. Note that the cdf of the source signals in practice is not known but needs to be estimated using nonlinear functions which closely resemble the cdf.

2. Negentropy

The negentropy technique derived in [10] uses information theory to maximize the non-Gaussianity of the estimated source signals under the assumption that the source signals are non-Gaussian and independent to start with. The approach relies on the fact that the pdf of a mixture of non-Gaussian random variables can only be closer to that of a Gaussian random variable than the mixture components can be as a result of the Central Limit Theorem. Negentropy is defined as the difference between the entropy of a random variable and the entropy of a variable with Gaussian distribution of the same variance, leading to

$$J_{neg}(y) = H(y_{gauss}) - H(y). \tag{11}$$

Unlike Infomax, where we evaluate the entropy of the transformed signal which is bounded in range, negentropy evaluates the entropy of the signal and, as a result, is constrained only by its mean and variance. In this case, the Gaussian distribution has maximum entropy [11]. Note that maximizing the non-Gaussianity of the source signals is achieved by maximizing the negentropy, as $H(y_{gauss})$ is constant for a fixed variance.

Both information-theoretical approaches described require knowledge of the pdf of the source signals. Since such information may not be available or may be too computationally expensive, nonlinear functions are usually used to approximate signal statistics implicitly [10].

3. Kurtosis Approach

Kurtosis-based methods are similar in objective to the negentropy approach by seeking to maximize the non-Gaussianity density of the estimated source signals but follow a different approach. In these methods, maximizing the non-Gaussianity property is achieved by searching for an un-mixing vector which maximizes the absolute value of the fourth-order marginal cumulant, commonly known as the kurtosis, directly for each source signal [12]. The kurtosis of a zero-mean random variable y is defined as

$$K(y) = E\{|y|^4\} - 2(E\{|y|^2\})^2 - |E\{y^2\}|^2, \tag{12}$$

where $E\{.\}$ represents the mathematical expectation. Note that when y is real the kurtosis simplifies to

$$K(y) = E\{y^4\} - 3(E\{y^2\})^2. \tag{13}$$

E. ICA LIMITATIONS

The first limitation of ICA is that variances of the source signals cannot be determined a priori. Since all we have available are the signal mixtures, any scaling factor in the source signals can become part of the mixing vectors thus causing uncertainty. Likewise, the phase and order of the extracted signals cannot be determined, as any permutation of the source signals can be offset by a permutation of the mixing matrix. Lastly, the source signals cannot all be Gaussian [11].

F. COMPLEX SIGNALS

In communications, signals are often modulated by one or more orthogonal basis functions in an effort to more efficiently use a given bandwidth. When doing so, the signal information can be encoded within the phase, frequency and amplitude of the baseband signal. The most common types of modulation use cosine and sine functions as the basis functions. For these types of modulation, also known as in-phase and quadrature phase or I-Q, it is easier to represent the phase and amplitude of those modulated signals with complex expressions. Therefore, plots of communication signals are often displayed in the complex plane through scatterplots of the real versus imaginary portions of the signal, known as signal constellation diagrams. A typical constellation diagram of a 16-level rectangular quadrature amplitude modulated (16-QAM) signal is shown in Figure 2.

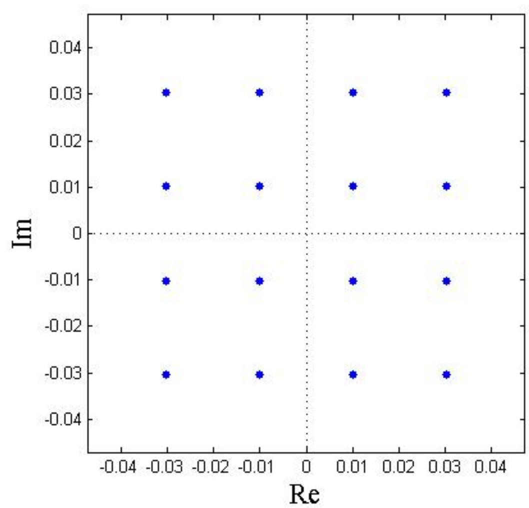

Figure 2. Constellation diagram of a 16-QAM signal.

Circularity is a property of a complex random variable describing the symmetry properties of its distribution [13]. A circular complex random variable has circular symmetry about the origin which is invariant for any phase rotation. Therefore, the pdf of a circular complex random variable z has the property

$$f(z) = f(e^{j\theta}z), \quad \forall\theta\in\mathbb{R}. \tag{14}$$

An example of a non-circular complex Gaussian random variable with different real and imaginary variances is shown in Figure 3.

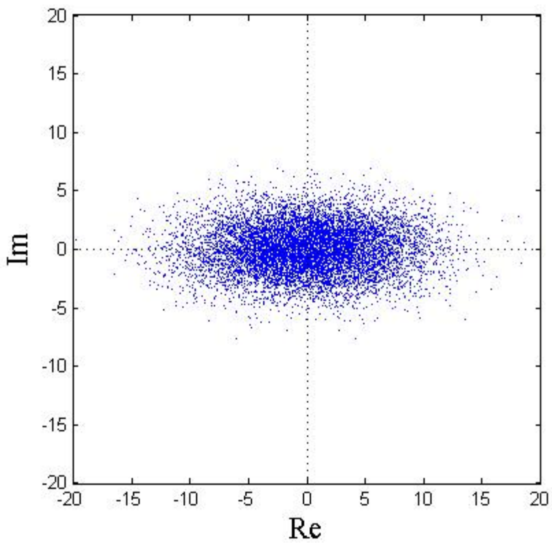

Figure 3. Example of a complex non-circular Gaussian random variable.

This circularity property is important in the extensions of the complex ICA algorithms to non-circular sources. This is due to the assumptions of circular sources, which simplified previous derivations of algorithms for complex sources. Take for instance the value of kurtosis shown in (12). If the random variable y is circular and has unit variance, the kurtosis reduces to

$$K(y) = E\{|y|^4\} - 2. \tag{15}$$

The particular expression in (15) is the cost function used in the kurtosis-based complex FastICA (cFastICA) algorithm designed to separate circular source signals [13].

To measure the circularity of a zero-mean complex random variable the circularity coefficient $|\rho|$ is used, where

$$\rho = \frac{E\{y^2\}}{E\{|y|^2\}}. \tag{16}$$

Likewise, the pseudo-covariance matrix can be used to measure the circularity for a set of signals. For a vector of zero-mean complex random variables $\mathbf{y}$, the pseudo-covariance matrix $\mathbf{P}$ can be estimated by

$$\mathbf{P}_{\mathbf{yy}} = \frac{1}{N}\sum_{n=1}^{N}\mathbf{y}(n)\mathbf{y}^{T}(n), \tag{17}$$

as opposed to the covariance matrix

$$\mathbf{C}_{\mathbf{yy}} = \frac{1}{N}\sum_{n=1}^{N}\mathbf{y}(n)\mathbf{y}^{H}(n). \tag{18}$$

A signal with a circularity coefficient of zero is called second order circular. Take for instance the 16-QAM signal shown in Figure 4. If this signal is phase shifted by some amount, the circularity coefficient is still zero, but the equal symmetry about the real and imaginary axis is no longer true. Therefore, the 16-QAM signal is considered to be only second order circular. An example is shown in Figure 4.

In the next chapter we will present source separation algorithms based on the criteria presented.

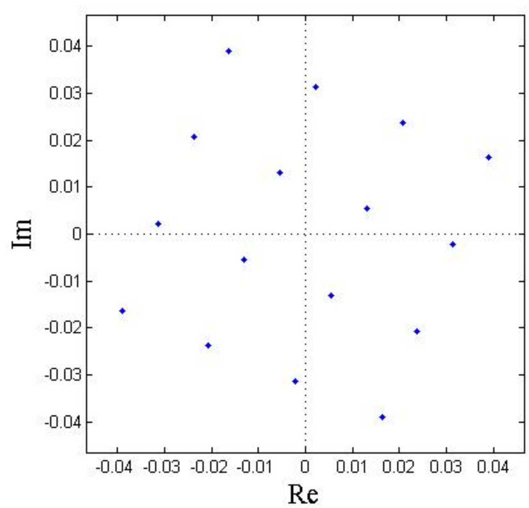

Figure 4. An example of a phase shifted 16-QAM signal showing second order circularity.

THIS PAGE INTENTIONALLY LEFT BLANK

III. ICA ALGORITHMS

In this chapter, we provide an overview of the three ICA algorithms used to extract the weak communication signal.

A. COMPLEX MAXIMIZATION OF NON-GAUSSIANITY (CMN)

The CMN algorithm is a modification of the cFastICA algorithm [10] and is based on the maximization of negentropy. For the complex case, the negentropy $J_{neg}(y)$ is the same as defined in Equation (11), but now y is a complex random variable:

$$J_{neg}(y) = H(y_{gauss}) - H(y). \tag{19}$$

The entropy $H(y_{gauss})$ of a complex Gaussian random variable y_{gauss} is constant for a fixed covariance; therefore, minimizing the differential entropy $H(y)$ leads to the maximum non-Gaussian source signal [10]. Instead of computing the pdf needed to calculate the entropy, cFastICA uses a nonlinear contrast function $G(y)$ to estimate the negentropy, which eliminates the need to perform an online estimate of $J_{neg}(y)$. The estimated source signal y can also be written in terms of the un-mixing vector $\mathbf{w}$ and the whitened signal mixtures $\mathbf{z}$ $(y = \mathbf{w}^H \mathbf{z})$. This leads to the algorithm cost function defined as

$$J_{FastICA}(\mathbf{w}) = E\{G(|\mathbf{w}^H \mathbf{z}|^2)\}, \tag{20}$$

where $\mathbf{z}$ contains the whitened signal mixtures. The CMN algorithm modifies this cost function by removing the modulus operation in the expression within the contrast function $G(.)$. This step preserves the signal phase information for source separation and allows for the use of asymmetric nonlinear contrast functions which match more closely the distributions of noncircular sources [6]. The adjusted cost function becomes

$$J_{CMN}(\mathbf{w}) = E\{\,|G(\mathbf{w}^H \mathbf{z})|^2\,\}. \tag{21}$$

This new cost function is used to derive the quasi-Newton or approximate Newton update of the algorithm to find the optimal un-mixing vector $\mathbf{w}$. The minimization step is done iteratively. Derivations for such implementation can be found in [6] and lead to

$$\mathbf{w}_{k+1} = -E\{G^*(y)g(y)\mathbf{z}\} + E\{g(y)g^*(y)\}\mathbf{w}_k + E\{\mathbf{z}\mathbf{z}^T\}E\{G^*(y)g'(y)\}\mathbf{w}_k^*. \tag{22}$$

The terms $g(y)$ and $g'(y)$ are the first and second order derivative of the contrast function $G(y)$, respectively, and $(.)^*$ represents the complex conjugate operation. Note this update is similar to that included in the cFastICA iteration but also includes the pseudo-covariance matrix of the whitened mixture $E\{\mathbf{z}\mathbf{z}^T\}$ in the third term, which contains the source signal circularity information [6].

When applying CMN, the signal mixtures are first prewhitened using singular value decomposition (SVD). The estimated source signals are then extracted sequentially after applying the algorithm to optimize the un-mixing vector. Finally, before each extraction, the un-mixing vector is made orthogonal to all previously found vectors to avoid extracting the same signal twice.

B. CFPA

The CFPA algorithm also extends from an alternate version of cFastICA [13] and uses the normalized fourth-order marginal cumulant as the cost function:

$$K(\mathbf{w}) = \frac{E\{|y|^4\} - 2(E\{|y|^2\})^2 - |E\{y^2\}|^2}{(E\{|y|^2\})^2}. \tag{23}$$

The cFastICA approach is best suited for second order circular signals, while the CFPA algorithm takes into account potential non-circular source properties with the assumption of prewhitened mixtures. The algorithm's iteration update is based on an approximate Newton optimization and is shown in [7] to be given by

$$\tilde{\mathbf{w}}_k = \left(\frac{1}{N}\sum_{n=1}^{N}|y(n)|^2 y(n)\mathbf{z}^*(n)\right) - 2\mathbf{w}_k - \hat{\mathbf{P}}^*\mathbf{w}_k^*\left[\mathbf{w}_k^T\hat{\mathbf{P}}\mathbf{w}_k\right], \tag{24}$$

where $\hat{\mathbf{P}}$ is defined as the pseudo-covariance matrix of the whitened mixtures. This is followed by a normalization step

$$\mathbf{w}_{k+1} = \frac{\tilde{\mathbf{w}}_k}{\sqrt{\tilde{\mathbf{w}}_k^H \tilde{\mathbf{w}}_k}}. \tag{25}$$

Again, the update is similar to that found in cFastICA, except for the third term which takes into account potential non-circular source properties [7]. The algorithm is applied in the same manner as in CMN and follows the same steps by prewhitening using SVD, sequential extraction, and sequentially orthogonalizing the resulting un-mixing vectors.

C. ROBUSTICA

The RobustICA algorithm is similar to the CFPA approach in that it uses the normalized kurtosis as the cost function; however, it differs in the optimization procedure. RobustICA employs an exact line search to determine the optimal step-size for a gradient descent procedure on the cost function. The optimal step-size has been shown to provide some robustness to local extrema and saddle points in the cost function [8]. The exact line search of the optimal step-size μ_{opt} is described by

$$\mu_{opt} = \arg\max_{\mu} | K(\mathbf{w} + \mu\mathbf{g}) |, \tag{26}$$

where and $K(.)$ is the updated kurtosis cost function and $\mathbf{g}$ is the gradient of the cost function. By the derivations shown in [8], it follows that

$$\mathbf{g} = \nabla_{\mathbf{w}} K(\mathbf{w}), \tag{27}$$

and

$$\nabla_{\mathbf{w}} K(\mathbf{w}) = \frac{4}{(E\{|y|^2\})^2}\left[E\{|y|^2 y^*\mathbf{x}\} - E\{y\mathbf{x}\}E\{y^{*2}\} - \frac{\left(E\{|y|^4\} - |E\{y^2\}|^2\right)E\{y^*\mathbf{x}\}}{E\{|y|^2\}}\right]. \tag{28}$$

The optimal step size is calculated by choosing the root of an optimal step size polynomial which provides the absolute maximum of the cost function in the search direction. The polynomial is derived from the signal mixtures along with the current iteration values of $\mathbf{w}$ and $\mathbf{g}$ [8]. Once the optimal step size is found, the un-mixing vector is updated by

$$\tilde{\mathbf{w}}_n = \mathbf{w}_n + \mu\mathbf{g} \tag{29}$$

and then normalized by

$$\mathbf{w}_{n+1} = \frac{\tilde{\mathbf{w}}_n}{\left\|\tilde{\mathbf{w}}_n\right\|}. \tag{30}$$

Although more computationally intensive per iteration, RobustICA benefits from overall faster convergence and, more importantly, does not require prewhitening of the data [8]. Again, the algorithm is applied procedurally in the same fashion as CMN and CFPA are when prewhitening is performed. However, when prewhitening is not performed, the estimated source signal is deflated from the signal mixtures before the extraction of the next signal in place of the orthogonalization step when prewhitening is implemented. Extraction still occurs sequentially.

IV. EXPERIMENTAL SETUP

The signal types considered and the procedures implemented to investigate the performances of the three ICA approaches in extracting the weak communication signal imbedded in White Gaussian noise from a high power broadcast signal are described in this section.

A. SOURCE SIGNALS

The co-channel interference scenario investigated in this work includes a weak communication signal imbedded in a high power TV broadcast signal in the presence of additive white Gaussian noise. The weak interfering communication signal of interest is assumed to be a BPSK, 4-QAM, or 16-QAM modulated signal generated from vectors of uniformly distributed random integers. Two TV broadcast standards are considered: North American standard, Advanced Television Systems Committee (ATSC), and European standard, Digital Video Broadcasting - Terrestrial (DVB-T).

1. ATSC Signal

The ATSC broadcast is an eight-level amplitude shift key (8-ASK) signal composed of data blocks with 259,584 message symbols and 706 data field synchronization symbols [14]. The 8-ASK signal is sub-Gaussian and non-circular, which can be seen in the signal constellation diagram of an ATSC signal shown in Figure 5.

2. DVB-T Signal

The DVB-T broadcast is an orthogonal frequency-division multiplexed (OFDM) signal. The standard allows for the operation of single or multiple frequency subcarriers modulated with 4-QAM, 16-QAM, or 64-QAM [15]. The input, whether a single signal broken into multiple data blocks or multiple signals, is assigned to multiple sub carrier frequencies and then undergoes an inverse discrete Fourier transform (IDFT). On the receiving end, the broadcasted signal is converted back to the source signals at the subcarrier frequencies with a fast Fourier transform (FFT).

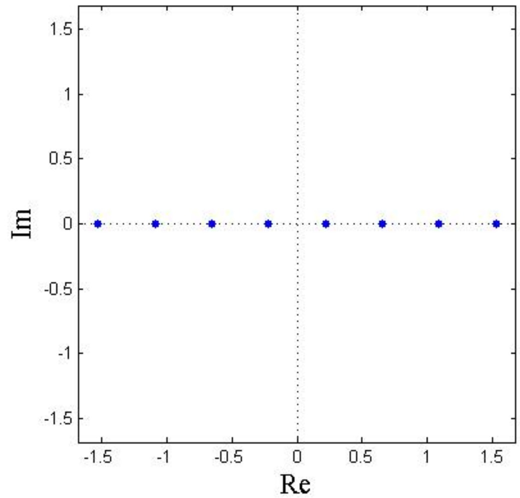

Figure 5. Signal constellation diagram of an ATSC signal of unit power and no noise.

In this work, we analyze the received signal before the FFT step is applied at the receiver end. At this point the received signal is approximately Gaussian in distribution and is nearly circular. The single signal 4-QAM, OFDM option was arbitrarily chosen for the simulations. Its constellation diagram is shown in Figure 6.

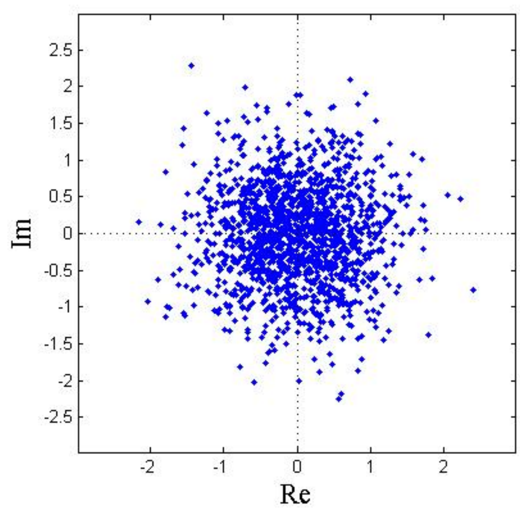

Figure 6. Signal constellation diagram of a DVB-T signal of unit power and no noise.

B. MIXTURE GENERATION MODEL

A description of the co-channel interference scenario used for the two-sensor case, as depicted in Figure 7, is provided in this section. The same process was followed when using larger numbers of sensors.

Three assumptions were made in the model. First we assumed the transmitters were not co-located and, therefore, traveled through separate channels for each sensor. Second, the set of sensors were relatively close in distance, which results in no signal attenuation. Lastly, we assumed a one-coefficient instantaneous channel scenario only, where all the channel complex coefficients have magnitude equal to 1.0 with a constant phase offset uniformly distributed between $-\pi$ and π.

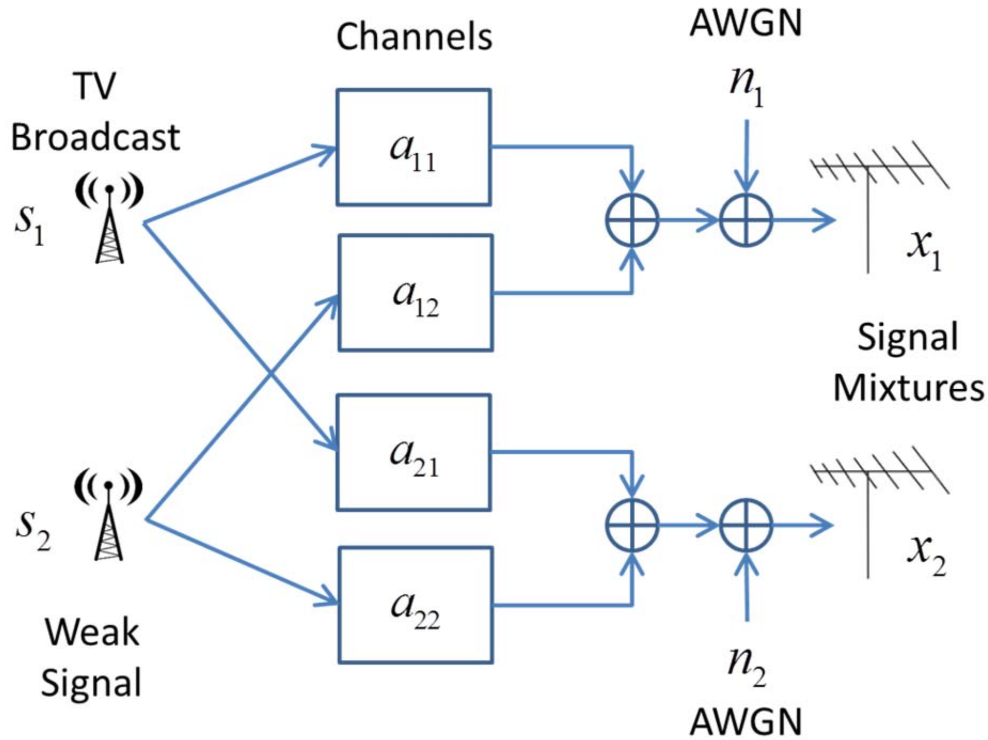

Figure 7. Co-channel interference model for two sensors.

Simulations were written and run in the MATLAB technical computing environment and signals and noise generated as follows.

- Data sets for the TV signals were generated from Simulink models in accordance with the associated ATSC and DVB-T standards described in [14] and [15], respectively. For each trial, a uniform random window of fixed length was applied to select a data set from a pre-generated ATSC or DVB-T signal consisting of roughly 1.75×10^6 points [19].
- The weak communication signal was generated from an array of uniform random integers using the appropriate modulation function within MATLAB for the signal type.
- The TV signal power-to-weak interfering signal power ratio (SIR) quantity was computed by first normalizing the power of the TV signal to 1.0 and then scaling the weak signal accordingly. Next, each signal was sent through the one-coefficient complex channel filters resulting in two filtered signals per sensor.
- The channel noise added to each sensor was generated with normally distributed complex random sequences, normalized, centered and then scaled to provide the desired weak interfering signal power-to-noise power ratio (INR) for each sensor.
- The pairs of filtered signals were then summed together with the noise resulting in a signal mixture for every sensor.

The k^{th} signal mixture x_k is a linear combination which fits the ICA model in (6) and is described by

$$x_k = a_{k1}s_1 + a_{k2}s_2 + n_k, \tag{31}$$

where a_{kj} is the mixing coefficient associated with source j and sensor k, s_j is a source signal, and n_k is the noise. An example of a mixture from an ATSC and 16-QAM with noise is shown in Figure 8, which shows a phase shift due to the wireless channel.

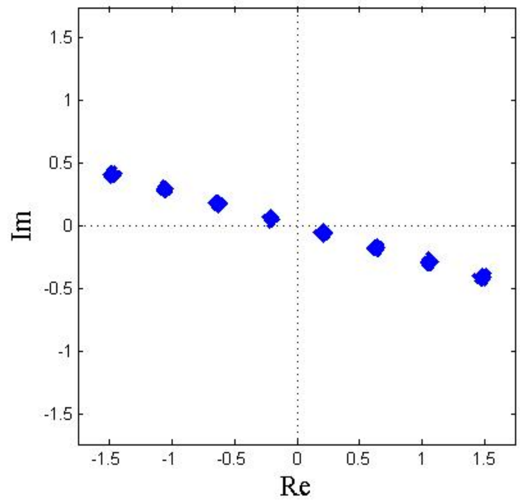

Figure 8. Mixture of an ATSC and 16-QAM signal with noise: 30 dB SIR, 10 dB INR, and 1000 samples.

After signal mixtures were generated, we applied the three ICA algorithms to extract the weak communication signal. As noted before in the limitations of ICA, the phase and order of the extracted signals cannot be determined. Therefore, in order to compute the symbol error rate of the recovered weak communication signal, the phase ambiguity had to be corrected. This was accomplished using the covariance between source signals and the extracted signals using a modified portion of the *compute_smse.m* function from the RobustICA software package found in [18] and available in the Appendix. This covariance matrix is used to search for extraction position of the estimated weak signal and then construct and apply a permutation and phase correction matrix in order to compare the extracted weak signal to the transmitted source signal.

The weak interfering signal was then demodulated using the corresponding *demodulate.m* function within MATLAB, and the symbol error rate (SER) was calculated with the default MATLAB symbol error rate function *symerr.m* [16]. An example of an extracted signal is shown in Figure 9.

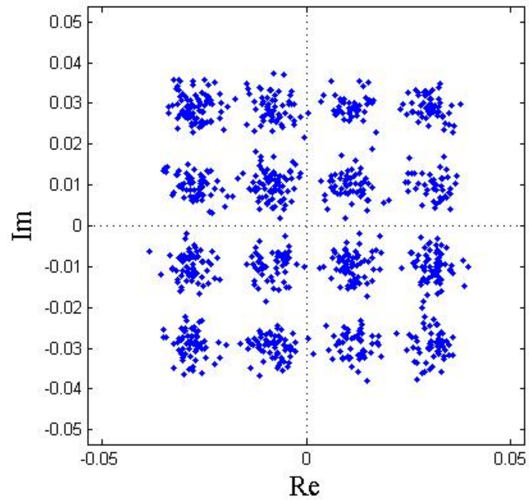

Figure 9. Extracted 16-QAM weak interfering signal using RobustICA: 30 dB SIR, 10 db INR, six sensors, 1000 samples, 3×10^{-3} symbol error rate, prewhitening step applied.

Most simulation runs, except when specified otherwise, are based on 10^4 trials run for a fixed SIR of 30 dB and INR values which range from –2 dB to 20 dB to ensure an adequate sample size. Recall, S is the broadcast and I refers to the weak signal. The ATSC standard requires a signal-to-noise ratio threshold of 28.3 dB, which led to the choice of the fixed SIR value of 30 dB. Different signal lengths were examined; however, data sets of 1000 samples were used in the majority of scenarios to improve the timeliness of the simulations and also provide performance insight if the algorithms were implemented in an adaptive model. The results will be discussed in Chapter V.

Performances obtained for each ICA implementation to extract the weak communication signal were investigated by computing the SER of the weak signal versus different INR levels. A 95% confidence interval (CI) for the SER was included in the results rather than a standard deviation as the symbol error rate does not exhibit Gaussian properties.

V. EXPERIMENTAL RESULTS

Performance results obtained to extract a weak communication signal imbedded in a TV broadcast signal in the presence of various levels of white noise distortion, where extraction performances were represented in terms of the SER level obtained for the estimated weak signal, are presented in this chapter. The simulations address a number of factors that impact the ability of the examined algorithms to extract the weak signal. These factors include the level of separation between instantaneous mixtures, the data length selected for processing, white noise level, and the number of sensors. Results show all three ICA algorithms performed identically for the two-signal, two-sensor case with noise, referred to as the basic case. However, this may not be the case in more complex implementations involving a larger number of antennas.

A. LEVEL OF SEPARATION BETWEEN MIXTURES IMPACTS

How the level of separation between the mixed signals and the noise level affects the quality of the recovered weak communication signal in the two-sensor case is investigated in this section.

In this scenario, the level of separation between the mixtures is varied by changing the phase value of one of the transmission channel complex coefficients. Specifically, all channel coefficients except one are fixed to 1.0, and the phase of the last coefficient (associated to one of the channels of the weak communication signal) was selected to be $\pi/8, \pi/2$, and π for various INR levels and a fixed SIR = 30 dB. Symbol error rates mean values obtained over 1500 trials at each INR level with associated 95% confidence intervals (CI) obtained for the RobustICA scheme with prewhitening are shown in Figure 10. Results show that the quality of the recovered weak signal improves as the channel coefficient phase angle increases, which is to be expected as the difference between mixtures increases with increasing phase angles. Note that same extraction performances were obtained for all three algorithms, and the RobustICA was arbitrarily chosen for presentation.

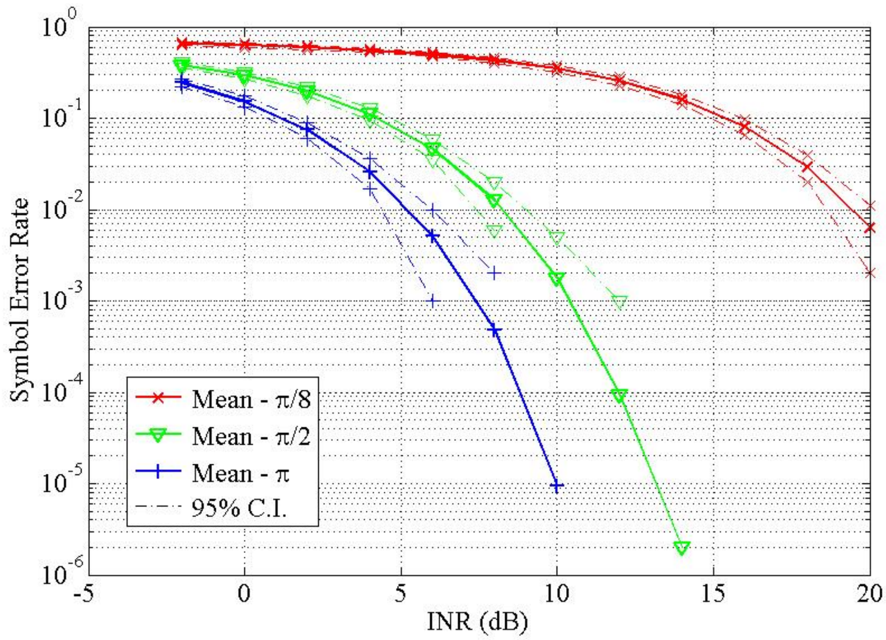

Figure 10. Impact of the channel phase angle difference for a 4-QAM signal extracted with RobustICA from an ATSC signal: two-sensor case, 1,000 data points, SIR = 30 dB, prewhitening step applied.

B. MEAN AND MEDIAN SER VALUES ISSUES

Note that both CI upper bound and lower bounds remain similarly close to the mean value in this scenario when the coefficient phase value difference is held fixed, as shown in Figure 10. However, such behavior disappears when all channel coefficient phase terms become randomized between $-\pi$ and π, as illustrated in Figure 11. Note in this case all the algorithms perform the same, and the results for the CMN algorithm may not be visible due to overlapping plots.

This change occurs as randomizing all channel phase coefficient values also introduces the possibility for these phase values to be close to each other for a given trial which leads to an ill-conditioned scenario, resulting in poor weak signal extraction and a high SER level at these specific trials. As a consequence, the CI upper bound obtained for the mean SER can be highly skewed due to few outliers.

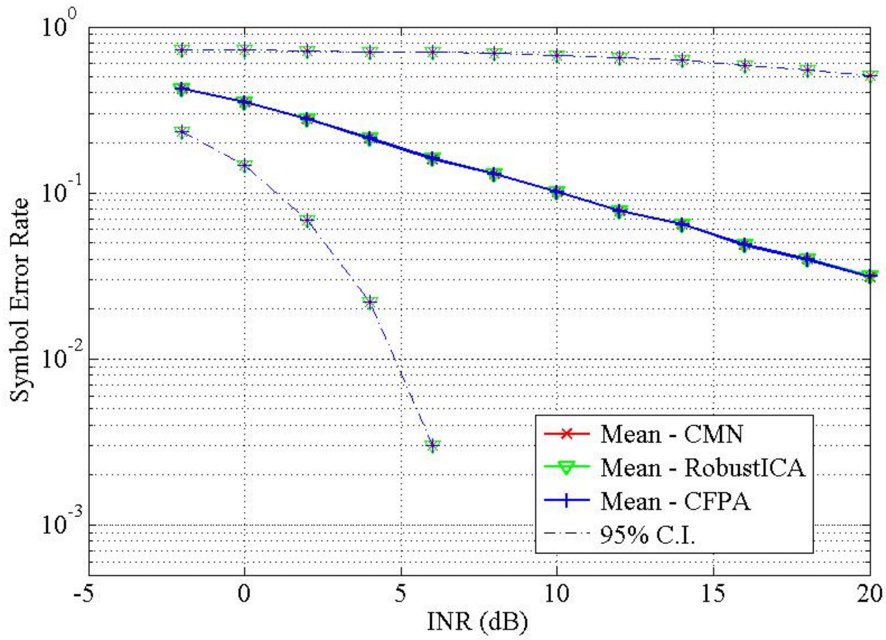

Figure 11. Mean SER for a 4-QAM signal extracted from an ATSC signal with all algorithms: two-sensor case, 1,000 data points, SIR = 30 dB, prewhitening step applied.

Let us consider a simulation experiment which includes 10^4 trials consisting of 1,000 data points per trial to further illustrate the impact outliers may have on resulting mean SER results. Note that at that data length, one symbol error results in a SER equal to 10^{-3}. Assume one trial leads to a SER equal to 0.10 and all other trails have SER levels equal to 0. In such a case, the mean SER of the overall simulation is equal to 10^{-5}, providing a distorted view for the overall performance. Note the median value is better suited to de-emphasize the impacts a few outliers have on a sequence overall behavior. As a result, median SER values and associated 95% CI levels were selected to evaluate the extraction performance in all other scenarios considered in this work instead of mean SER values.

Finally, note that our results present only symbol errors rates obtained for the recovered weak communication signals. However, the corresponding bit error rate (BER) is not computed, as we made no assumption regarding a particular error correction coding scheme. It is worth mentioning that most modern modulation schemes employ Gray coding when mapping symbols to the signals space, which results in the closest

neighboring symbols differing by only one bit. Also, the closest neighboring symbols errors are the likeliest to occur when dealing with AWGN distortions. Therefore, the BER is expected to be lower than the SER. For example, the BER obtained for 16-QAM modulation which has four bits per symbol, is expected to be roughly one-fourth of the SER value in reasonable noise environments. Employing error correction coding would further reduce the BER for a given SER.

C. CMN CONTRAST FUNCTIONS

The impact of different nonlinear contrast functions $G(y)$ were investigated in the CMN algorithm implementation. Results show choosing $G(y) = y^2$ as the contrast function provided the best overall extraction performance of the weak signal, followed by $\cosh(y)$ and $y^{0.25}$. Results for these three contrast functions to extract a 16-QAM signal are shown in Figure 12 for the six-sensor case. It is worth noting that we specifically used

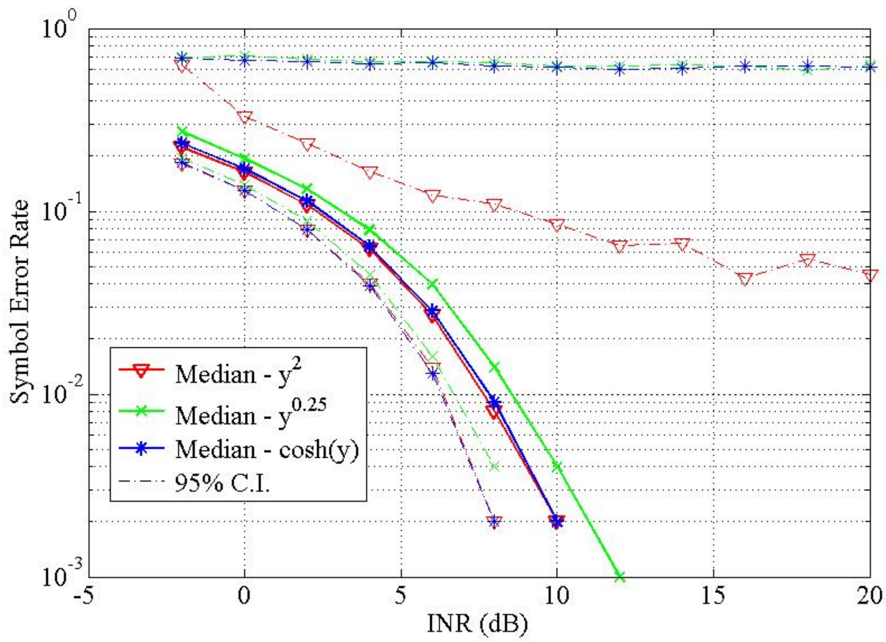

Figure 12. 16-QAM weak communication signal extracted using the CMN in the presence of a DVB-T signal using different contrast functions: six-sensor case, 1,000 data points, SIR = 30dB.

the y^2 contrast function for the remaining simulations as it led to better extraction performances over other contrast functions.

D. IMPACTS OF THE DATA LENGTH

Various data lengths from 100 to 10^5 were selected with no significant extraction performance differences for the two-sensor case. However, simulations showed the data length had a significant impact on resulting extraction performances for the CMN algorithm as the number of sensors increased, as illustrated in Figure 13 for the eight-sensor case and the ATSC broadcast signal type. Note higher CI upper bound levels indicate that the number of poorly recovered communication signal sequences increases when the data length is shortened from 10^5 to 1,000 in the eight-sensor case. This behavior was not observed for the other algorithms for the eight-sensor case with the ATSC broadcast type.

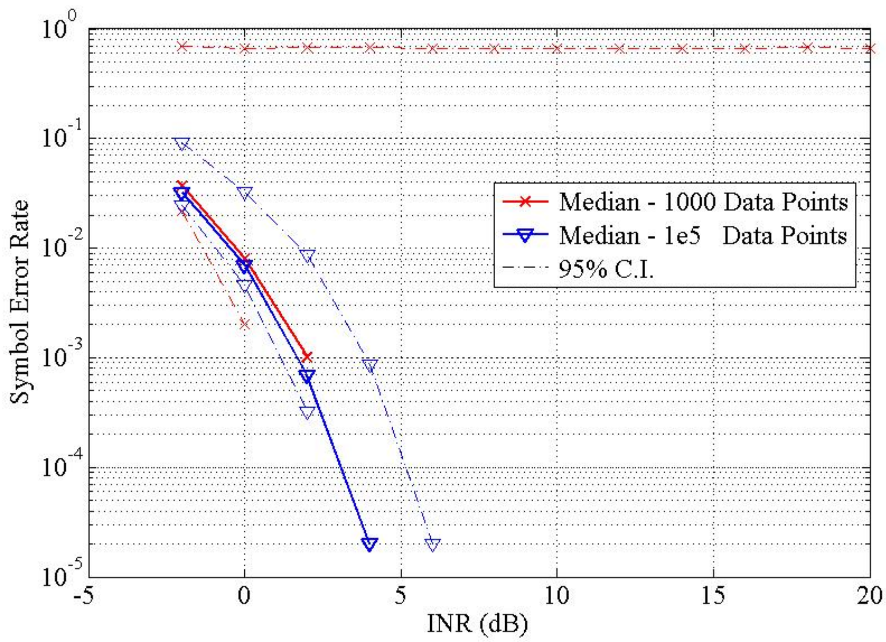

Figure 13. 4-QAM signal extracted with CMN from an ATSC signal: eight-sensor case, different length data with SIR = 30dB.

Novey, et al. noted that the CMN algorithm can become unstable for non-circular sub-Gaussian sources when using the y^2 contrast function, leading to poor extraction

performance, as illustrated from the upper bound for CMN in Figure 14 [6]. Also, recall that the ATSC signal is non-circular. Such behavior is not as noticeable (a lower CI upper bound) when the CMN is applied to the more circular DVB-T signal, as shown in Figure 15.

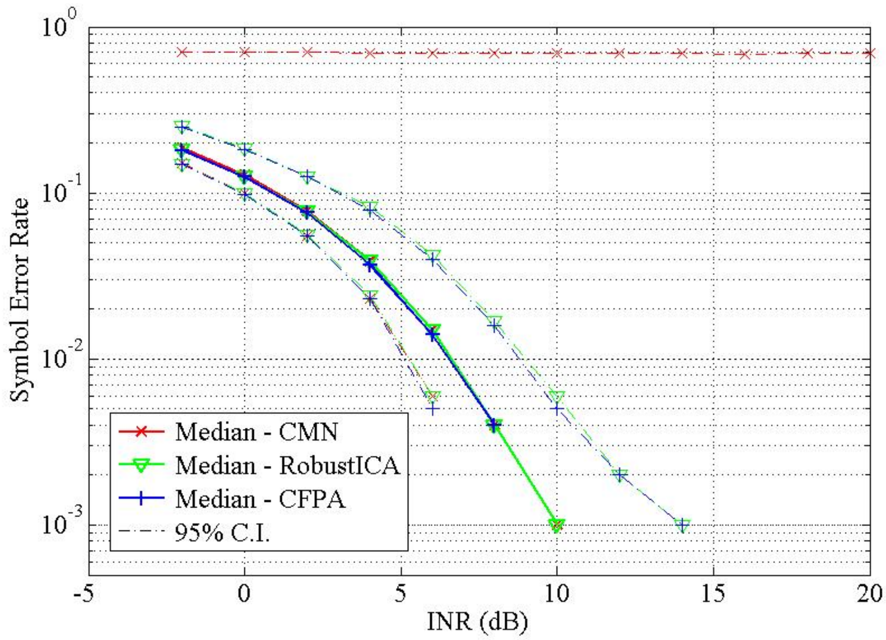

Figure 14. 16-QAM signal extracted from an ATSC signal using all algorithms: eight sensor case of 1,000 data points with SIR = 30 dB. Prewhitening step present in RobustICA implementation.

However, when the DVB-T broadcast type is used, the data length also affects the overall performance of the CFPA and RobustICA algorithms when a prewhitening step is applied. For simulations of 1500 trials and eight-sensors, the difference in extraction performance of a 16-QAM weak signal can be seen for RobustICA in Figure 16 and CFPA in Figure 17. Testing higher number of sensors for larger number of data lengths was prohibitive due to simulations run times.

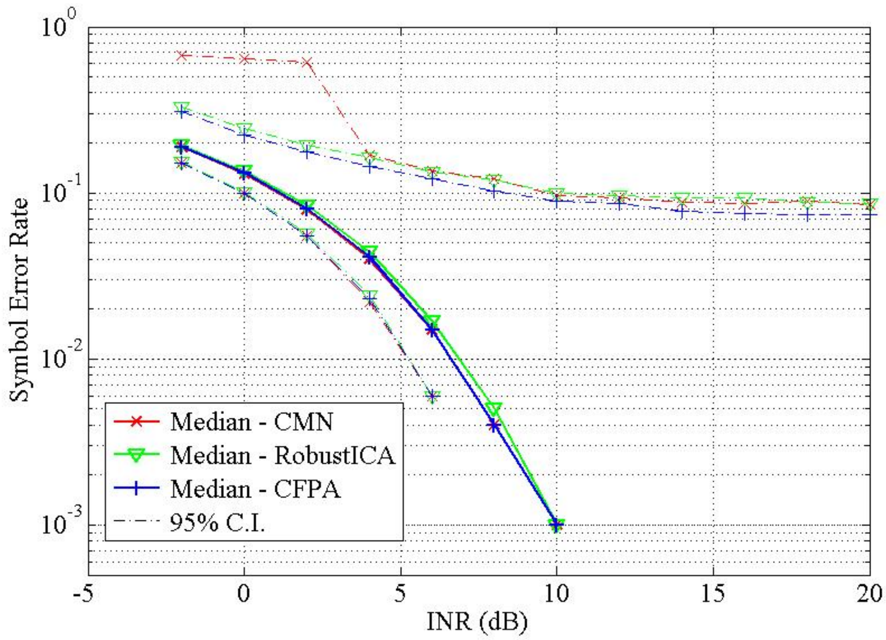

Figure 15. 16-QAM signal extracted from a DVB-T signal using all algorithms: eight sensor case of 1,000 data points with SIR = 30 dB. Prewhitening step present in RobustICA implementation.

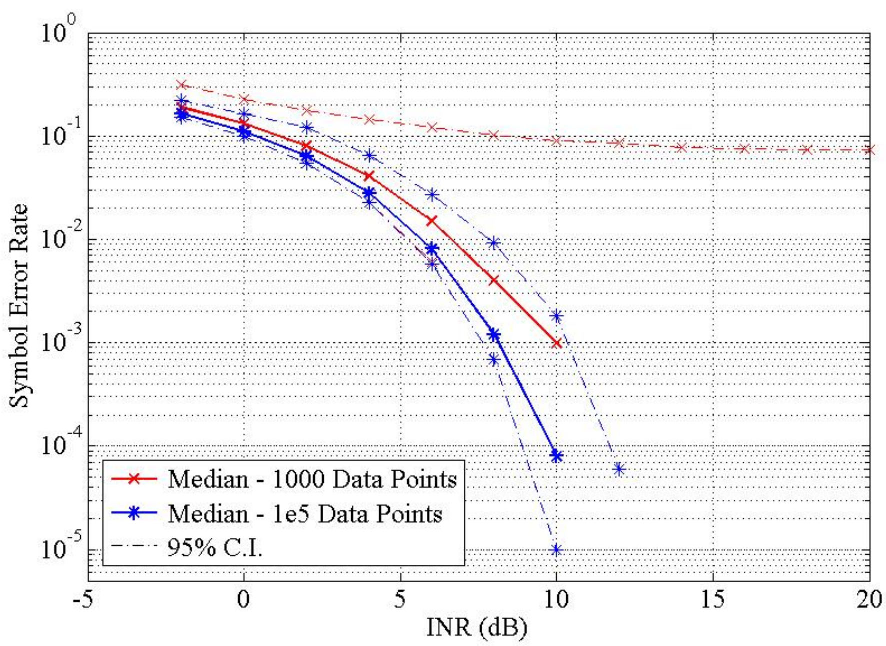

Figure 16. 16-QAM signal extracted with CFPA from a DVB-T signal: eight-sensor case, different length data with SIR = 30 dB.

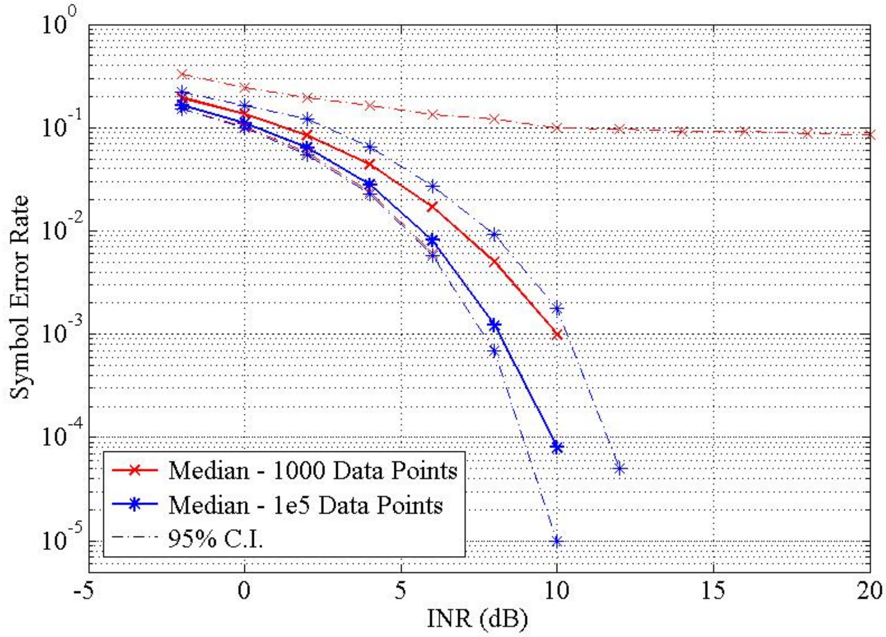

Figure 17. 16-QAM signal extracted with RobustICA from a DVB-T signal: eight-sensor case, different length data, SIR = 30 dB, prewhitening step applied.

E. ESTIMATED SIGNAL EXTRACTION ORDER

Recall that the ICA schemes considered in this work are iterative in nature, i.e., they successively extract signal components present in the mixtures one after the other. Also, recall that ultimately only the weak communication signal is of interest here, and it is desirable to stop the extraction process as quickly as possible, as there is no benefit in extracting noise components. Thus, the order in which the communication signal and the TV broadcast signal are extracted as the number of sensors increases is investigated in this section. A simulation of 3×10^6 trials was run to extract the weak signal for the scenario of four sensors, SIR = 30 dB, and INR = 7 dB for all algorithms and both broadcast types. Results show that the two signals of interest are extracted before the noise components, as illustrated in Tables 1 and 2. Specifically, results indicate that the weak communication signal is always successfully extracted as one of the first two components except in cases where the recovery quality is too poor to be considered successful. Findings for the ATSC TV broadcast case, which is non-Gaussian in nature, is summarized in Table 1. Note that in this case, the ATSC signal is the highest power non-Gaussian signal and is extracted first with the weak communication signal extracted

second. Findings for the DVB-T TV broadcast case, which behaves closely to a Gaussian signal, is summarized in Table 2. In this case, the weak communication signal is the most non-Gaussian and is extracted first. However, smaller data sets of the DVB-T are slightly sub-Gaussian and will occasionally be extracted first due to their higher power. The distributions of the DVB-T signal are shown in Figure 18 for the full data set and in Figure 19 for a window of 1,000 samples.

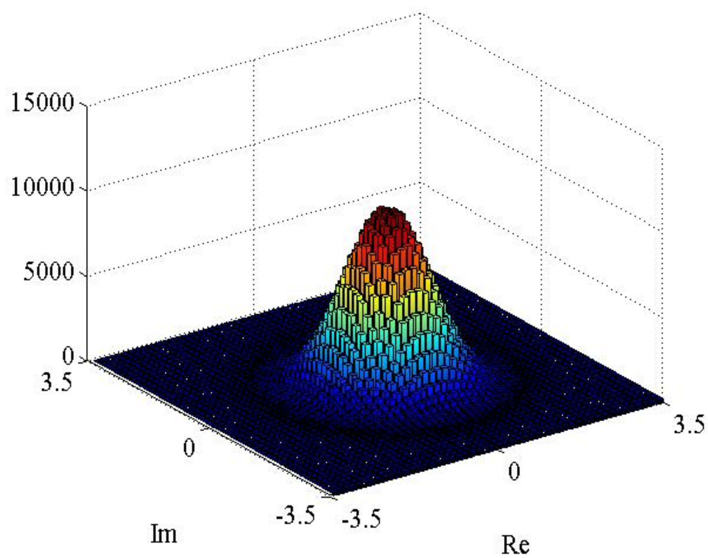

Figure 18. Distribution for full data set of the DVB-T signal.

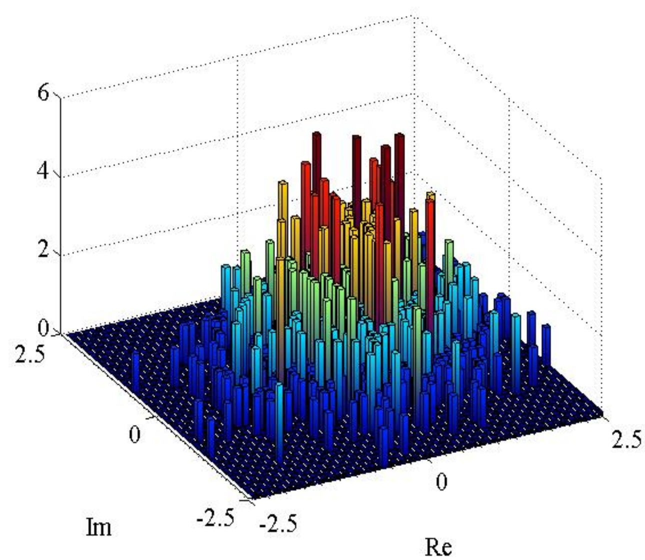

Figure 19. Distribution for 1000 samples of the DVB-T signal.

Again all three ICA algorithms behaved the same when a prewhitening step was applied in each, and the RobustICA was arbitrarily chosen for presentation. Thus, ICA algorithms were stopped after the extraction of the first two signals in cases where more than two sensors were used.

Table 1. The weak communication signal extraction order for a 4-QAM signal from an ATSC signal using RobustICA at SIR = 30 dB, INR = 7 dB, four sensors, and a prewhitening step applied.

	Times extracted in position	% of Total Trials	Symbol Error Rate		
			Mean	Min.	Max
Position 1	0.0	0.0	0.0	0.0	0.0
Position 2	2.999E+06	99.95	0.005	0.000	0.741
Position 3	789	0.026	0.559	0.316	0.734
Position 4	660	0.022	0.586	0.405	0.740
Total	3.00E+06				

Table 2. The weak communication signal extraction order for a 4-QAM signal from a DVB-T signal using RobustICA at SIR = 30 dB, INR = 7 dB, four sensors, and a prewhitening step applied.

	Times extracted in position	% of Total Trials	Symbol Error Rate		
			Mean	Min.	Max
Position 1	2.96E+06	98.648	0.0047	0	0.734
Position 2	39,259	1.309	0.0690	0	0.729
Position 3	686	0.023	0.5792	0.378	0.739
Position 4	601	0.020	0.5965	0.413	0.741
Total	3.00E+06				

F. WHITE GAUSSIAN NOISE IMPACTS

We also investigated the impact of Gaussian white noise distortion added to the mixtures on the performance of the ICA algorithms in extracting the weak signal.

Results show that the extraction of the weak signal occurs without errors at signal-to-interference ratios ranging from –50 to 60 dB for a two-channel case and no noise for all three ICA algorithms. Note this scenario corresponds to the proper mixture scenario, i.e., the same number of signals and channels. The same behavior is seen when the number of sensors increases to three and the same noise is present in each channel, giving a total of three mixtures and three source signals.

When different white Gaussian noise distortion sequences are present in each channel, the problem can be viewed as underdetermined by a ratio of K:(K+2), where K is the number of sensors. On the other hand, when the number of sensors increases without the presence of noise, the problem becomes overdetermined to a ratio of K:2. In the latter case, when the mixtures are prewhitened, all three algorithms become numerically unstable and fail to extract the weak inferring signal even in a scenario of three sensors and two signals of 1000 data points. When the mixtures do not undergo a prewhitening step, extraction using RobustICA occurs with only minor errors for cases of high number of sensors and no noise.

G. NUMBER OF SENSORS IMPACTS

Up to eight sensors were considered for the various types of communication and broadcast signal to examine the impact of increasing the amount of sensors has on the weak signal extraction performance.

A simulation of 10^4 trials was run to extract the weak signal for the scenario of two, four, and eight sensors, SIR = 30 dB, and INR from –2 to 20 dB for all algorithms and both broadcast types. As the number of sensors increases, results show that the quality of the extracted weak communication signal increases for the three ICA algorithms investigated. The outcome for CFPA is shown in Figures 20 and 21, which was the same for all algorithms when a prewhitening step is applied.

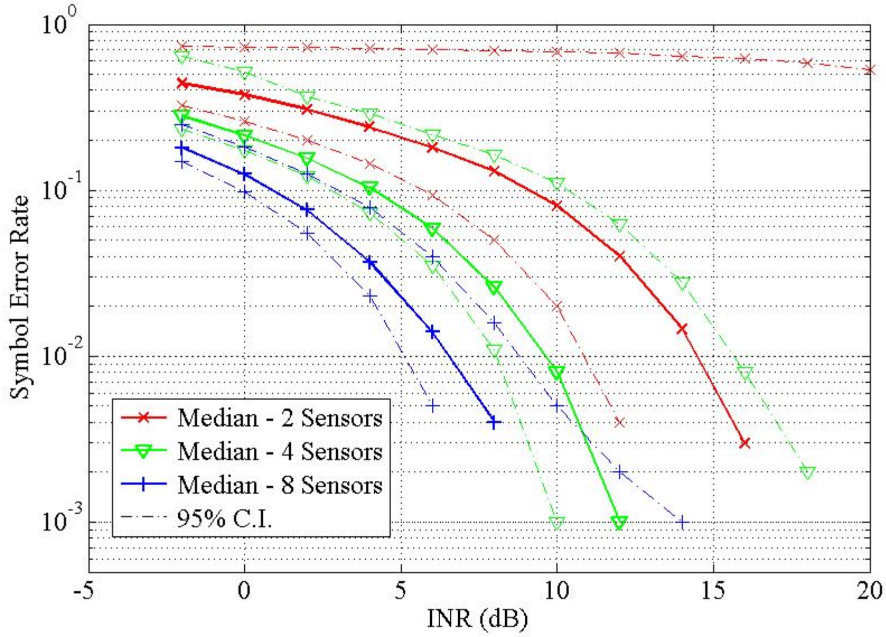

Figure 20. 16-QAM signal extracted with CFPA from an ATSC signal. Different sensor cases of 1,000 data points with SIR = 30 dB.

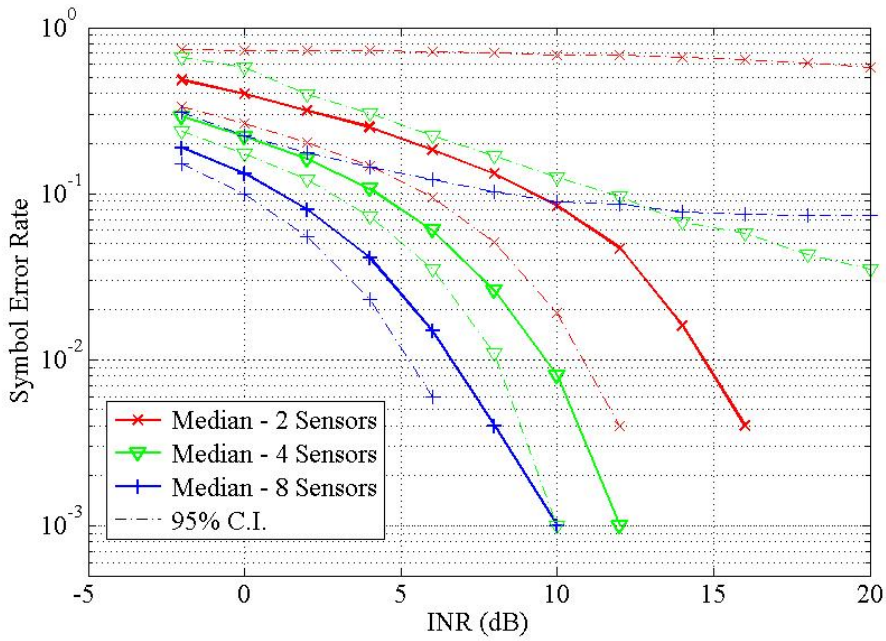

Figure 21. 16-QAM signal extracted with CFPA from a DVB-T signal. Different sensor cases of 1,000 data points with SIR = 30 dB.

H. IMPACT OF PREWHITENING

The results pertaining to the upper bounds in Figure 15 also highlight another issue concerning the performances of the examined ICA algorithms. Recall this was the scenario of the 16-QAM extracted from a DVB-T signal with eight sensors where the upper bound did not improve as the noise level decreased. The effects of noise stated earlier become a factor in the scenarios with large numbers of K sensors. At lower noise levels, i.e., higher INR values, the underdetermined K:(K+2) problem tends to behave as the over-determined K:(2) problem which may lead to ill-conditioned behavior when a prewhitening step is first applied. Therefore, a cross-over point exists for the gain in extraction performance when increasing the amount of sensors for a given INR. In the cases where large number of sensors is used and low noise is present, a small amount of noise could be added to improve ICA extraction stability or the number of available mixtures reduced after the prewhitening step. Although there is a slight reduction in extraction performance, this instability is not seen when the mixtures are not prewhitened, as shown in Figure 22. This can only be accomplished with the RobustICA algorithm since it was derived without the assumption prewhitened mixtures unlike CMN and CFPA.

I. WEAK SIGNAL TYPES

When the levels of modulation of the weak interfering signal are lowered, i.e. 16-QAM to 4-QAM, the energy per symbol increases relative to the noise, and the symbol error rate decreases as expected. The performance of RobustICA to extract the three analyzed types of weak signals with four sensors is shown in Figures 23 and 24. The other examined ICA algorithms provide nearly identical results.

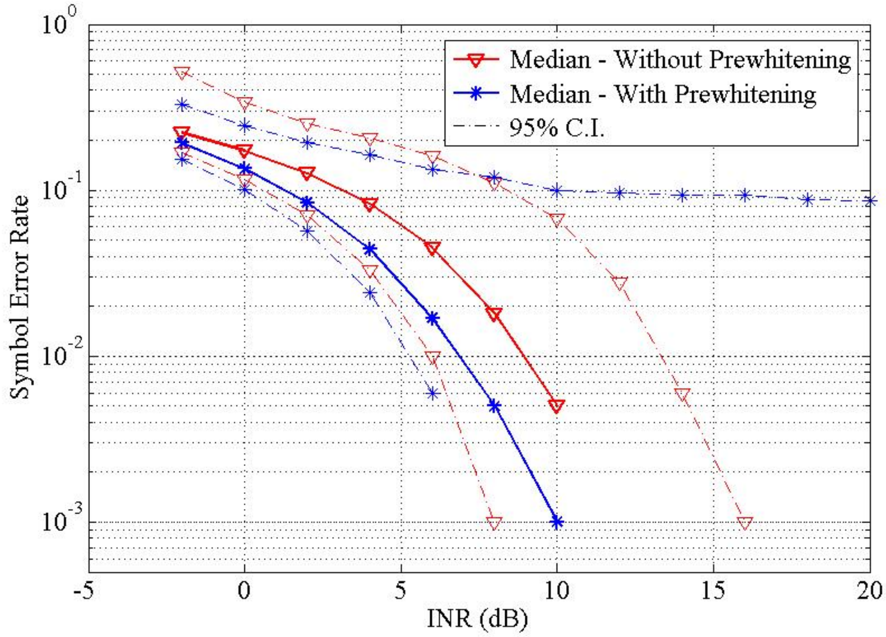

Figure 22. 16-QAM signal extracted from a DVB-T signal using RobustICA with and without a prewhitening step. Eight sensor case of 1,000 data points with SIR = 30 dB.

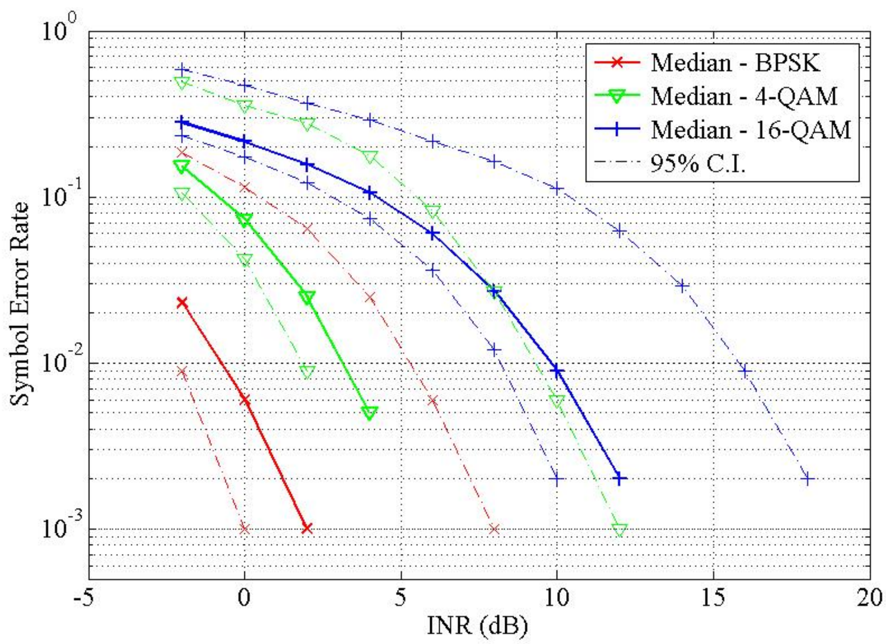

Figure 23. Different signal types extracted with RobustICA from an ATSC signal. Four sensor case of 1,000 data points, SIR = 30dB, and a prewhitening step applied.

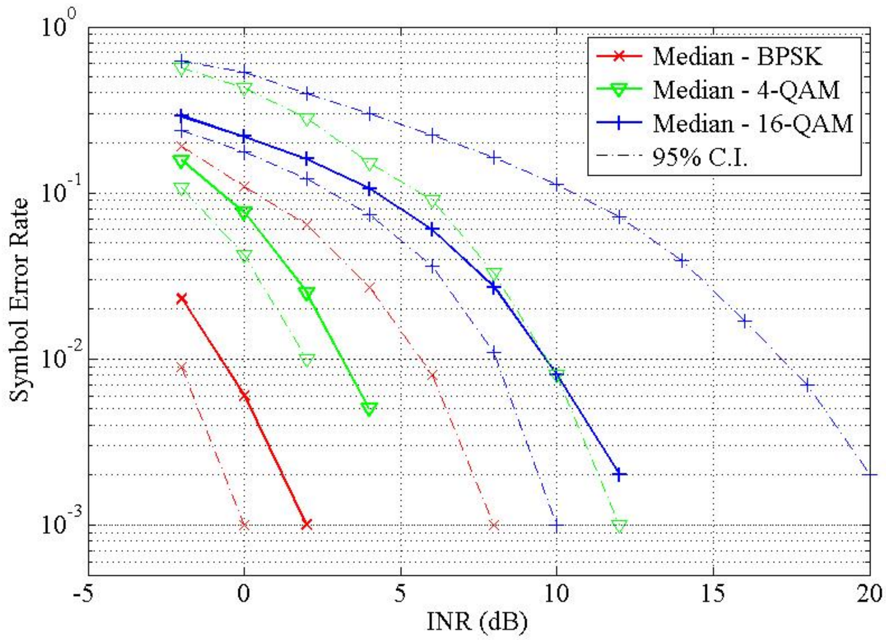

Figure 24. Different signal types extracted with RobustICA from a DVB-T signal. Four sensor case of 1,000 data points, SIR = 30dB, and a prewhitening step applied.

THIS PAGE INTENTIONALLY LEFT BLANK

VI. CONCLUSIONS

The ability for complex ICA algorithms to extract a weak communication signal embedded in the same channel of a TV broadcast was investigated in this thesis. Three ICA algorithms were selected, and their performances in extracting the weak signal in the presence of high power TV broadcast signal and additive white Gaussian noise were investigated. Specific ICA implementations considered were complex maximization of non-Gaussianity (CMN) by Adali et al. [6], the complex fixed-point algorithm (CFPA) by Douglas [7], and the RobustICA by Zarzoso et al. [8].

A. SUMMARY OF RESULTS

Overall results show ICA as a viable option to extract a weak co-channel interfering communication signal imbedded in a high power TV broadcast signal and white Gaussian noise with no multipath. Findings show extraction performance is influenced by the amount of signal mixture separation, the level of noise present, the number of sensors used, and the application of a prewhitening step.

Weak signal extraction occurs best with maximum separation between observed signal mixtures. Results show better extraction is obtained as the number of sensors increases. However, results also show the prewhitening step may also lead to degraded extraction performance when more than two sensors are used or there is little to no noise. In these cases an ICA algorithm which does not necessarily require a prewhitening step, such as RobustICA, may be the best suited for weak signal extraction.

Findings also show the performance of all three algorithms improves as the level of modulation for the weak signal type decreases.

B. RECOMMENDATIONS FOR FUTURE WORK

Recommendation for improvements and further study include the following: expansion of the model to incorporate multipath fading, translating the current algorithms and model into Simulink for real-time continuous simulations, and sensor array optimization to maximize the separation of the observed signal mixtures for varying transmitter locations.

THIS PAGE INTENTIONALLY LEFT BLANK

APPENDIX

The MATLAB code used evaluate the extraction performance is provided in this appendix. The complete code, including functions and modified algorithms, are available upon request from the author (mehagste@nps.edu) or thesis advisor (fargues@nps.edu). The original MATLAB code for the three algorithms evaluated are available in [7], [17], and [18].

A. MATLAB CODE FOR SIMULATION

```
%%% EXTRACTION OF A WEAK CO-CHANNEL INTERFERING COMMUNICATION SIGNAL
%%% USING COMPLEX ICA
%
% Author: Matthew Hagstette

clear; clc; close all;

%% User input
INR_db=10;          % Weak signal to noise power ratio
SIR_db=30;          % TV to Weak signal power ratio
Ndata=1000;         % Length/Number of samples for ATSC signal
n_chan=4;           % Number of Sensors/Number Channels for each signal
Nsources_only=2;    % Number of signals to extract
  % Weak channel attenuation, max percent difference: 0.2 = +/-10%
weak_atten=0;
  % TV channel attenuation, max percent difference: 0.2 = +/-10%
TV_atten=0;
phase_restrict=0;   % Restrict random phase of all channels
  % Duration of one weak signal symbol, in terms of number of samples
L=1;
s_type='16QAM';     % Weak signal type ('4QAM','16QAM','QPSK','BPSK')
multipath=0;
iopt=10;            %% ICA options : 10 - All
                         %         :  1 - CMN
                         %         :  2 - Robust ICA
                         %         :  3 - CFPA
tol_CMN = 1e-6;          % termination threshold parameter: CMN
  % maximum number of iterations per independent component: CMN
max_it_CMN = 1e3;
tol_Rob = 1e-6;          % termination threshold parameter: RobustICA
  % maximum number of iterations per independent component: RobustICA
max_it_Rob = 1e3;
tol_CFPA = 1e-6;         % termination threshold parameter: CFPA
  % maximum number of iterations per independent component: CFPA
max_it_CFPA = 1e3;

%% Generate Channel Mixtures
```

```matlab
[ATSC_data]=load('atscdata');  % Load Pregenerated ATSC signal

  % Randomly select Ndata samples of TV signal
window_start = ceil(rand*(length(ATSC_data.transmitted_data)-
(Ndata+1)));
TVtrans_data = ATSC_data.transmitted_data(1, ...
                                    window_start:window_start+Ndata-1);

  % Send transmitted TV signal through "n_channel" number of channels
[TVrec_data] = ATSC_data_multi_chan_atten( TVtrans_data, multipath,...
                                    n_chan, phase_restrict, TV_atten );

  % Generate and Send weak signal through "n_channel" channels
[Wtrans_data, Wrec_data] = Weak_data_multi_chan_atten_ATSC( s_type, ...
     multipath, Ndata, L, n_chan, SIR_db, phase_restrict, weak_atten );

  % Transmitted signals
S.data=[TVtrans_data;Wtrans_data;zeros((n_chan-2),Ndata)];

  % Plot
figure;
Sp=S;Sp.data=S.data.';            % Rows to columns for plotting
[coldim,rowdim]=plotdata(Sp,'s'); % Scaterplots of transmitted signals
subplot(rowdim,coldim,1),title('Source Signals');

%% Generate Noise
[N,M]=size(Wrec_data);
S_p=diag(cov(Wrec_data.'));
k_noise=sqrt(S_p).*10^(-(INR_db/20));
K_noise=repmat(k_noise,1,M);
W0=randn(N,M)+1i*randn(N,M);
W0=W0-repmat(mean(W0,2),1,M);
W0=W0./(repmat(std(W0,0,2),1,M));
Noise=K_noise.*W0;

%% Observed Channel mixtures
X.data = TVrec_data+Wrec_data+Noise;

  % Plot
figure;
Xp=X;Xp.data=X.data.';            % Rows to columns for plotting
[coldim,rowdim]=plotdata(Xp,'x'); % Display Scatterplots: mixed signals
subplot(rowdim,coldim,1),title('Mixed Channels');


%%%% Alogrithm Calls %%%%

%% CMN Algorithm
if iopt==1 || iopt==10 ,  %(Option: Run CMN Algorithm )

    [Y1.data_r] = doCMNseq_reduced_modprewhite(X.data,'x^2',0, ...
                                   tol_CMN, max_it_CMN, Nsources_only);

      % Correct phase ambiguity and permutation
    [Y1.data,comm_pos] = reorder_norm(Y1.data_r, S.data);
```

```
      % Plot
    figure;
    Y1p=Y1;Y1p.data=Y1.data.';            % Rows to columns for plotting
      % Scatterplots of extracted signals
    [coldim,rowdim]=plotdata(Y1p,'y_1');
    subplot(rowdim,coldim,1),title('CMN')

      % Calculate errors
    [~,~, nsymerr, rsymerr] = error_calc_weak(Y1.data,S.data,s_type);
    nSym_Err(1,1)=nsymerr;
    rSym_Err(1,1)=rsymerr;
    Comm_Pos(1,1)=comm_pos;

end         %(End: CMN Algorithm Option)


%% RobustICA Algorithm

if iopt==2 || iopt==10 ,   %(Option: Run RobustICA Algorithm)

    [Y2.data_r] = robustica_reduced(X.data,[-ones(1,6),zeros(1,M-6)]...
              ,tol_Rob, max_it_Rob, 1, 'o', 0, [], 1,Nsources_only);

      % Correct phase ambiguity and permutation
    [Y2.data,comm_pos] = reorder_norm (Y2.data_r, S.data);
      % Plot
    figure;
    Y2p=Y2; Y2p.data=Y2.data.';           % Rows to columns for plotting
      % Scatterplots of extracted signals
    [coldim,rowdim]=plotdata(Y2p,'y_2');
    subplot(rowdim,coldim,1),title('RobustICA')

      % Calculate errors
    [~,~, nsymerr, rsymerr] = error_calc_weak( Y2.data,S.data,s_type);
    nSym_Err(2,1)=nsymerr;
    rSym_Err(2,1)=rsymerr;
    Comm_Pos(2,1)=comm_pos;

end         %(End: Robust ICA Algorithm Option)


%% CFPA Algorithm

if iopt==3 || iopt==10 ,  %(Option: Run CFPA Algorithm)
    [Y3.data] = CFPA_reduced_modprewhite(X.data.', tol_CFPA,...
                                       max_it_CFPA, Nsources_only);
    Y3.data_r=Y3.data.';
      % Correct phase ambiguity and permutation
    [Y3.data,comm_pos] = reorder_norm (Y3.data_r, S.data);
      % Plot
    figure;
    Y3p=Y3; Y3p.data=Y3.data.';           % Rows to columns for plotting
      % Scatterplots extracted signals
    [coldim,rowdim]=plotdata(Y3p,'y_3');
    subplot(rowdim,coldim,1),title('CFPA');
```

```
      % Calculate errors
    [~,~, nsymerr, rsymerr] = error_calc_weak( Y3.data,S.data,s_type);
    nSym_Err(3,1)=nsymerr;
    rSym_Err(3,1)=rsymerr;
    Comm_Pos(3,1)=comm_pos;
end         %(End: CFPA Algorithm Option)
```

B. MATLAB CODE FOR PERMUTATION AND PHASE CORRECTION OF THE EXTRACTED WEAK SIGNAL

```
function [Se,Comm_Pos] = reorder_norm (Se, S)
% OUPTPUT:
%
%    Se  : re-ordered, phase corrected and scaled estimate
%
%    Comm_Pos: Determines if comm signal is pulled first, 1 = yes
%
% INPUTS:
%
%    S  : actual sources (one source per row)
%
%    Se : estimated source signals (one source per row)
%
% reorder_norm.m is a modification of the "greedy" algorithm described
% in Section IV.A of  V. Zarzoso and P. Comon,
% <a href = "http://www.i3s.unice.fr/~zarzoso/biblio/tnn10.pdf">
% "Robust independent component analysis by iterative maximization</a>
% <a href = "http://www.i3s.unice.fr/~zarzoso/biblio/tnn10.pdf">
% of the kurtosis contrast with algebraic optimal step size"</a>,
% IEEE Transactions on Neural Networks, vol. 21, no. 2,
% pp. 248-261, Feb. 2010.
%
% Sept 2012 - modified to handle over-determined case,
% and weak extraction position

[n, T] = size(S);

  %% Perform optimal ordering (via "greedy algorithm"),
  %% as well as scaling and phase correction

S_std=std(S,0,2);

Se_std=std(Se,0,2);

C_std=S_std*Se_std.';

C_std( find(C_std==0) )= eps;

   % estimated signal amplitudes for scaling
ampe_dist = sqrt( diag( Se*Se') / T);

C = 1/T*S*Se';                    % spatial cross-correlation matrix
Cabs = abs(C);
```

```
Cnorm = Cabs./C_std;
D = zeros(n, n);                % scale matrix
Ph = D;                         % phase correction matrix
P = D;                          % permutation matrix

for k = 1:n;
    if norm(Cnorm) ~= 0
        % poslin = row #s of max value in each column
    [maxlin, poslin] = max(Cnorm);
        % poscol = column # of max value in Matrix Cabs
    [~, poscol] = max(maxlin);
        % original source   = row # of max value in Matrix Cabs
    orgsrc = poslin(poscol);
        % estimated source  = column # of max value in Matrix Cabs
    estsrc = poscol;
        % optimal scaling in the MMSE sense
    D(orgsrc, orgsrc) = Cabs(orgsrc, estsrc)/ampe_dist(estsrc)^2;
        % phase: related to 'sign' of correlation
    Ph(orgsrc, orgsrc) = sign(C(orgsrc, estsrc));
    P(orgsrc, estsrc) = 1;      % permutation
        % do not refer to that estimated source anymore
    Cnorm(:, estsrc) = zeros(n, 1);
        % do not refer to that original source either
    Cnorm(orgsrc, :) = zeros(1, n);

    else    % Permutation fill for signals with XCorr = 0
        [~, prow] = min(sum(P,2));
        [~, pcol] = min(sum(P,1));
        P(prow, pcol) = 1;
        Ph(prow,prow)=1;
        D(prow,prow)=1;
    end % end if
end % for k

% get estimated sources ready for comparison

Se = Ph*D*P*Se;
[~,Comm_Pos]=max(P(2,:));  % Determines order weak signal pulled

end   % end function
```

THIS PAGE INTENTIONALLY LEFT BLANK

LIST OF REFERENCES

[1] A. Hyvärinen, J. Karhunen, and E. Oja, *Independent Component Analysis.* New York, NY: John Wiley & Sons, pp. 11–12, 2001.

[2] A. J. Bell and T. J. Sejnowski. “An information-maximization approach to blind separation and blind deconvolution,” *Neural Computation,* vol. 7, no. 6, pp. 1129–1159, Nov. 1995.

[3] P. Comon, “Independent component analysis, a new concept?” *Signal Processing*, vol. 36, no. 3, pp. 287–314, 1994.

[4] A. Hyvärinen and E. Oja, “A fast fixed-point algorithm for independent component analysis,” *Neural Computation*, vol. 9, no. 7, pp. 1483–1492, Oct. 1997.

[5] A. Cichocki, S. Amari, *Adaptive Blind Signal and Image Processing*. New York, NY: John Wiley & Sons, pp. 24–32, 2002.

[6] M. Novey and T. Adalı, “Complex ICA by negentropy maximization,” *IEEE Trans. Neural Networks*, vol. 19, no. 4, pp. 596–609, Apr. 2008.

[7] S. C. Douglas, “Fixed-point algorithms for the blind separation of arbitrary complex-valued non-Gaussian signal mixtures,” *EURASIP Journal on Advances in Signal Processing*, DOI: 10.1155/2007/36525, 2007.

[8] V. Zarzoso and P. Comon, “Robust independent component analysis by iterative maximization of the kurtosis contrast with algebraic optimal step size,” *IEEE Trans. Neural Networks*, vol. 21, no. 2, pp. 248–261, Feb. 2010.

[9] A. Hyvärinen, J. Karhunen, and E. Oja, “Principal Component Analysis and Whitening,” in *Independent Component Analysis*. New York, NY: John Wiley & Sons, pp. 125–144, 2001.

[10] A. Hyvärinen, “Fast and robust fixed-point algorithms for independent component analysis,” *IEEE Trans. Neural Networks*, vol. 10, no. 3, pp.626–634, 1999.

[11] A. Hyvärinen and E. Oja. “Independent component analysis: algorithms and applications,” *IEEE Trans. Neural Networks*, vol. 13, no. 4, pp. 411–430, Apr. 2000.

[12] E. Bingham and A. Hyvärinen, “A fast fixed-point algorithm for independent component analysis of complex valued signals,” *Int. J. Neural Syst.*, vol. 10, pp. 1–8, 2000.

[13] E. Ollila, V. Koivunen, H. V. Poor, "Complex-valued signal processing — essential models, tools and statistics," Information Theory and Applications Workshop (ITA), 2011, pp.1–10, DOI: 10.1109/ITA.2011.5743596, Feb. 2011.

[14] "ATSC Digital Television Standard—Part 2: RF/Transmission System Characteristics," ATSC A/53, Dec. 2011.

[15] "Digital Video Broadcasting (DVB); Implementation Guidelines for DVB Terrestrial Services; Transmission Aspects," ETSI TR 101 190 v1.3.2, May 2011.

[16] The MathWorks. "The Mathworks–Support," [Online]. Available: http://www.mathworks.com/support

[17] CMN algorithm [Online]. Available: http://mlsp.umbc.edu/codes/TCMNsym.m [Accessed: May 2013].

[18] RobustICA algorithm [Online]. Available: http://www.i3s.unice.fr/~zarzoso/robustica.html [Accessed: May 2013].

[19] R. Cristi. (Fall 2012). ATSC and DVB-T signal generation. [Personal Correspondence.] Naval Postgraduate School, Monterey, CA.

INITIAL DISTRIBUTION LIST

1. Defense Technical Information Center
   Ft. Belvoir, Virginia

2. Dudley Knox Library
   Naval Postgraduate School
   Monterey, California